

UNCLASSIFIED

AD 274 320

*Reproduced
by the*

**ARMED SERVICES TECHNICAL INFORMATION AGENCY
ARLINGTON HALL STATION
ARLINGTON 12, VIRGINIA**



UNCLASSIFIED

NOTICE: When government or other drawings, specifications or other data are used for any purpose other than in connection with a definitely related government procurement operation, the U. S. Government thereby incurs no responsibility, nor any obligation whatsoever; and the fact that the Government may have formulated, furnished, or in any way supplied the said drawings, specifications, or other data is not to be regarded by implication or otherwise as in any manner licensing the holder or any other person or corporation, or conveying any rights or permission to manufacture, use or sell any patented invention that may in any way be related thereto.

274320

ACTIA

CAT. NO. 10

274 320

NEUTRON DOSIMETRY, SPECTROMETRY, AND NEUTRON ACTIVATION ANALYSIS

Theos J. Thompson
Norman C. Rasmussen
Daniel Schwartz

554 500

Massachusetts Institute of Technology
77 Massachusetts Avenue
Cambridge, Massachusetts

FINAL REPORT
MIT - NE 8

Contract No. AF 19(604)-3461
Project 5620
Task 56206

October 1961

62-3-1

Electronics Research Directorate
Air Force Cambridge Research Laboratories
Office of Aerospace Research
United States Air Force
Bedford, Massachusetts

Neutron Dosimetry, Spectrometry, and
Neutron Activation Analysis

Theos J. Thompson
Norman C. Rasmussen
Daniel Schwartz

Massachusetts Institute of Technology
77 Massachusetts Avenue
Cambridge, Massachusetts

FINAL REPORT

MIT-NE 8

Contract No. AF 19(604)-3461

Project 5620

Task 56206

October 1961

Electronics Research Directorate
Air Force Cambridge Research Laboratories
Office of Aerospace Research
United States Air Force
Bedford, Massachusetts

Requests for additional copies by Agencies of the Department of Defense, their contractors, and other Government agencies should be directed to the:

ARMED SERVICES TECHNICAL INFORMATION AGENCY
ARLINGTON HALL STATION
ARLINGTON 12, VIRGINIA

Department of Defense contractors must be established for ASTIA services or have their 'need-to-know' certified by the cognizant military agency of their project or contract.

All other persons and organizations should apply to the:

U. S. DEPARTMENT OF COMMERCE
OFFICE OF TECHNICAL SERVICES
WASHINGTON 25, D. C.

ABSTRACT

A thorough investigation of the leakage spectrum from the MITR has been carried out using the MITR fast chopper. These measurements have been made for three different fuel loadings, in the energy range from 0.001 ev to 10 Kev. They have been compared with several theoretical models and are in fairly close agreement with the heavy gas model. A semiconductor neutron spectrometer is described that will be used for high energy spectrum measurements.

A triple coincidence pair spectrometer designed for high efficiency is described. Calibration results using Na^{24} are reported. Operation of a six meter bent quartz crystal spectrograph for capture γ ray measurements is described. Preliminary results for the energies of seven Sc^{45} γ rays are 296, 229, 228, 217, 148, 143, 52 Kev. More accurate numbers will be available when final analysis of plates has been completed. Modification and construction of three different irradiation systems is described. These include modifications of the pneumatic rabbits to allow short half life work. Construction and operation of a vertical sample changing system and a ball sample changing system for longer irradiations are described.

TABLE OF CONTENTS

INTRODUCTION	1
CHAPTER I	
A. Measurement of Neutron Energy Spectra with the M.I.T. Fast Chopper	3
1. General	3
2. Equipment	4
3. Data handling	6
4. Results	7
a. General	7
b. Rotor Transmission	7
c. Neutron energy spectra	8
5. Conclusion	10
B. Semiconductor Neutron Spectrometer	11
1. General	11
2. Construction	11
C. Slow Chopper	13
CHAPTER II	
A. Investigations of Prompt Capture γ Ray Spectra	13
1. General	13
2. Triple Coincidence NaI Pair Spectrometer	14
a. Theory of Operation	14
b. Description	15
c. Performance	15
d. Future studies	16
3. Bent Quartz Crystal Spectrometer	16
B. Prompt α Analysis for Boron	16
C. Irradiation Facilities	17
1. Pneumatic rabbits	17
a. General	17
b. Rabbit Configurations	18
c. Rabbit Temperatures	19
d. Rabbit Fluxes	20
2. Vertical Facility	22
3. Ball Sample Changer	23
D. Irradiations	24
REFERENCES	25

INTRODUCTION

The principle aims of the research started under this contract are twofold. The first is to develop and evaluate techniques for measuring neutron spectra for inter-reactor calibration and spectrometry. The second aim is to develop new techniques in the general field of activation analysis with particular attention to identification of impurities in electronic materials.

During the first year we have concentrated on developing experimental equipment and facilities necessary for carrying out a broad program of research in these two areas. In the neutron spectroscopy area it was decided to make an effort to determine the spectrum of neutrons from a reactor port with high accuracy. A port whose spectrum is well known can then be used to check and evaluate various types of neutron spectrometers. In order to carry out this measurement a fast chopper already available was installed and put into operation at the 12" port of the MITR. This work is reported in Chapter I.A. In order to carry these results to higher energy, work is currently progressing on a semiconductor neutron spectrometer. Progress is described in Chapter I.B.

In the area of activation analysis it was decided to concentrate on techniques involving direct use of the reactor since it is so readily available. Work has been started in two areas. The first includes investigations to evaluate the feasibility of using the prompt radiation that follows neutron capture. Principle effort has been on developing methods for measuring prompt capture γ 's, although some work has been done on evaluating boron concentration by prompt α emission. A triple coincidence pair spectrometer and a bent quartz crystal spectrometer have been developed and recently put into operation at the reactor. This work is described in Chapter II.A.

INTRODUCTION

The principle aims of the research started under this contract are twofold. The first is to develop and evaluate techniques for measuring neutron spectra for inter-reactor calibration and spectrometry. The second aim is to develop new techniques in the general field of activation analysis with particular attention to identification of impurities in electronic materials.

During the first year we have concentrated on developing experimental equipment and facilities necessary for carrying out a broad program of research in these two areas. In the neutron spectroscopy area it was decided to make an effort to determine the spectrum of neutrons from a reactor port with high accuracy. A port whose spectrum is well known can then be used to check and evaluate various types of neutron spectrometers. In order to carry out this measurement a fast chopper already available was installed and put into operation at the 12" port of the MITR. This work is reported in Chapter I.A. In order to carry these results to higher energy, work is currently progressing on a semiconductor neutron spectrometer. Progress is described in Chapter I.B.

In the area of activation analysis it was decided to concentrate on techniques involving direct use of the reactor since it is so readily available. Work has been started in two areas. The first includes investigations to evaluate the feasibility of using the prompt radiation that follows neutron capture. Principle effort has been on developing methods for measuring prompt capture γ 's, although some work has been done on evaluating boron concentration by prompt α emission. A triple coincidence pair spectrometer and a bent quartz crystal spectrometer have been developed and recently put into operation at the reactor. This work is described in Chapter II.A.

The second area of investigation is an activation analysis using short half life materials. Before a program in this area could begin it was necessary to modify and calibrate the existing pneumatic rabbit system and construct a hot cell. In addition to rabbit modifications two other types of irradiation systems have been constructed. All this work is described in the last part of Chapter II.

CHAPTER I

A. Measurement of Neutron Energy Spectra with the M.I.T.R. Fast Chopper

(C. A. Anderson)

1. General

The primary objective of this work was to establish a means of examining neutron spectra emanating from reactors and by using this to investigate typical neutron spectra from the M.I.T. Reactor. Subsidiary uses planned for the completed apparatus included measurement of total neutron cross sections and capture gamma ray studies.

The reason for carrying out studies of neutron energy spectrum measurements is that the calculation of spectra is very unreliable for any reactor system which is heterogeneous, has non $1/v$ absorption, is not a monatomic gas, or which has finite dimensions - consequently any practical reactor system.

Because of the unsatisfactory nature of calculational methods, full sized or nearly full sized assemblies called critical assemblies are often built to check these calculations. However, critical assembly studies at best yield only crude information about neutron energy spectra, typically by the use of foil detectors.

It is possible, however, to measure the energy dependent flux at any location in the nuclear reactor core by taking a sufficiently large portion of this core as a subcritical assembly, bombarding it with source neutrons, and measuring the resultant flux.

The neutron beam from a given point in the lattice (preferably near the center) may be extracted through a re-entrant thimble, collimated, and then pulsed by a rotating shutter. The neutrons are detected at the end of a fixed flight path and the resulting pulses deposited in the proper channel of a multi-channel analyzer according to the neutron time-of-flight. The resulting number of neutrons per unit flight time is then converted to a neutron current per unit energy interval which is

typical of the lattice rather than of the neutron source used.

The first experiment of this type to be made at the M.I.T. Reactor was the measurement of the spectrum of neutrons leaking from the core tank of the reactor into the 12-inch horizontal port. In addition to being of basic interest to the study of reactor spectra the measurement is of interest to others who utilize this type of reactor. Because the reactor is cylindrically symmetrical the neutrons leaking into the dozen or more experimental facilities around the core have a similar energy spectrum. Hence knowledge of this neutron energy spectrum will prove useful to other experimenters at the M.I.T. Reactor and at other reactors of this general type.

Time of flight neutron spectrometers were first used for pulsed cyclotron neutron sources. The applicable equations are

$$E = \frac{5150}{(\tau/m)^2} \quad (1)$$

$$\text{and} \quad \frac{\Delta E}{E} = -0.0279 \frac{\Delta \tau}{m} \sqrt{E} + 2 \frac{\Delta m}{m} \quad (2)$$

Where E = neutron energy, ev

τ = flight time, μsec

m = flight path, m.

Figure 2 shows the energy resolution, $\Delta E/E$, which this equation yields for the MITR fast chopper. This figure shows that if the rotor is run at speeds of 100, 400, 900, 3000, and 7000 rpm, the maximum error in energy below 100 ev is less than 5%. Above 100 ev the $E^{1/2}$ law prevails, resulting in an energy resolution of 30% at about 5 kev. This sets the high energy limit of the system. The low energy limit is determined by the lowest speed attainable by the chopper rotor. With going into details, the low speed limit of 100 rpm allows measurement of spectra in the energy range down to about 4×10^{-3} ev and well below the most probable velocity of the Maxwellian spectrum.

2. Equipment

In August of 1959 a fast neutron chopper was purchased by M.I.T. from the Chr. Michelsens Institute, Norway. The

purchase consisted of the chopper rotor, vacuum enclosure, and a speed control system which included motors and generators. The remainder of the system was designed and built by the author during the succeeding year and one half.

It was decided at the outset that the primary use of the system would be for neutron energy spectrum measurements, although the design was to provide latitude for other experiments such as neutron cross section and capture gamma ray studies. This decision guided the design of the fast chopper ensemble.

Starting at the reactor end of the ensemble (Figure 1) the neutrons used in an experiment are coarsely collimated by a 1-inch diameter hole in the center of the 12SH1 shielding plug, then finely collimated by 13-1/2 inches of lead to a beam 0.031 inch x 1 inch. The neutrons enter the vacuum enclosure by means of a thin aluminum window and are further collimated by 1-1/4 inches of polystyrene to a beam 0.020 inch by 1 inch. When the chopper rotor slits align with the collimator, bursts of neutrons are passed thru another window to the outlet collimator (which serves merely to reduce background), and traverse a long helium filled bag, striking a bank of sensitive neutron detector tubes in an outhouse in the rear yard of the reactor.

When a chopper slit is aligned with the inlet collimator a burst of light is produced which is used to indicate zero time for the multichannel analyzer. The signal from the neutron detectors, created by a 6000 volt potential across each tube, is amplified and sent to the multichannel analyzer in the reactor building. The pulses produced in the neutron detectors occur at varying times after the zero time signal and are stored according to arrival time.

A cadmium covered neutron detector placed in masonite near the lead inlet collimator serves as a powermonitor and provides accurate normalization of data independent of reactor power changes. Additional equipment includes radiation and explosion shielding, enclosures for the helium bag and for detection ~~apparatus~~ and a system of gages and interlocks to prevent damage should excessive speed, vibration, temperature or vacuum chamber pressure be indicated.

3. Data handling

Seventy-four experimental runs were made, each consisting of 256 numbers. Handling such copious amounts of data is difficult and time consuming unless use is made of a high speed electronic computer. To measure the neutron energy spectrum the number of neutrons per unit flight time are counted. The count must be corrected for:

1. counts lost in analyzer due to deadtime,
2. integrated reactor flux-time during the experiment,
3. background,
4. detector efficiency,
5. neutron removal along the flight path, and
6. chopper rotor transmission.

The resultant number per unit flight time must then be converted to a current per unit energy.

The following equation summarizes this process:

$$J(E) = \frac{\tau^3 \left\{ \frac{RC(i)}{POW \left[1 - \frac{1}{B} \sum_{j=1}^{i-1} RC(j) \right]} - SWB \right\} \left\{ 1 - \frac{[G(i) - SWB] \left[1 - \frac{1}{B} \sum_{j=1}^{i-1} RC(j) \right]}{RC(i)} \right\}}{CONST \cdot X(\tau\omega) \cdot ABS(\tau) \cdot \eta(\tau)}$$

(This equation applies for $i \leq \frac{16}{W}$, a similar equation satisfies $i > \frac{16}{W}$)

where $RC(i)$ = counts recorded in channel i

POW = power normalization factor

B = number of neutron bursts during experiment

τ = flight time corresponding to channel i , μsec .

S = energy independent background constant, approx.
 1.1×10^{-6} counts/ μsec /burst.

$G(i)$ = counts in channel i for thick foil resonance transmission experiment.

$X(\tau\omega)$ = rotor transmission function.

ω = rotor speed, radians/sec.

$ABS(\tau)$ = neutron absorption along beam path

$\eta(\tau)$ = neutron detector efficiency

W = width of channel i , μsec .

E = energy, ev

$J(E)$ = neutron current per unit energy, $n/\text{cm}^2\text{-sec-ev}$.

This equation is solved by the IBM709 computer for each of the pieces of data generated by the multichannel analyzer. An auxiliary calculation is that of the total neutron cross section of a sample, given by

$$\sigma(E) = \frac{\tau^3}{10,453.6t} \ln \frac{N_1(i)}{N_2(i)}$$

where $\sigma(E)$ = cross section, cm^2/ev

$N_1(i)$ = counts in channel i , sample in

$N_2(i)$ = counts in channel i , open beam

t = sample thickness, atoms/cm^2

4. Results

Three series of experiments were run, namely:

Series I. No fuel in front of 12" port.

II. One fuel element in front of 12" port.

III. Two fuel elements in front of 12" port.

a. General

In addition to measuring the spectra, cross sections were measured and the energy scale of the multichannel analyzer was calibrated during the first series of experiments. The second and third series were devoted almost exclusively to spectrum measurement (including background measurement).

Resonance absorber foils of Cd, In, Au, and Co were used for both the energy calibration and for the determination of energy dependent background. That portion of the background not dependent on energy was measured by using a thick block of polyethylene to remove neutrons from the beam.

The cross section of palladium was measured in the energy range 5×10^{-3} ev to 20 ev and is shown in Figure 3. The agreement with the published curve of BNL-325 is good. The data shown was taken at rotor speeds of 130, 385, 850 and 3050 rpm, and the overlap of these various runs is good. The resonance indicated at 3 ev has not been reported elsewhere. Mr. Schweitzer and Mr. Teich made the measurement of the palladium cross section as their S.B. thesis in physics at M.I.T. (Reference 6)

b. Rotor Transmission

The rotor transmission function was measured by the use of the equation:

$$X_1(\tau\omega_1) = \frac{C_1(\tau, \omega_1)}{C_2(\tau, \omega_2)} X_2(\tau\omega_2)$$

where X_1 = rotor transmission at $\omega = \omega_1$

ω = rotor speed, rad/sec

τ :: neutron flight time

$C_1(\tau, \omega_1)$ = corrected count rate per channel at flight
time τ and $\omega = \omega_1$

It is possible to determine the rotor transmission from this equation by solving it for several values of τ and ω_1 for a fixed $\tau\omega_2$. The rotor transmission function must be correct in order for the data at different rotor speeds to result in the same neutron spectrum. This criterion of compatibility between runs may be used to correct an incorrect rotor transmission function.

c. Neutron energy spectra

When the previously mentioned calculations are performed, the neutron energy spectra shown in Figures 4, 5, and 6 are obtained. At high energies all the experimental points are shown, but as the energy decreases the points become indistinguishable on a graph; hence as few as 20% of the experimental points are shown at very low energy. The curves drawn on these three figures represent the Maxwellian distribution and the dE/E distribution which best fit the data. The effective neutron temperature of the Maxwellian distribution and the energy at which the dE/E slowing down distribution crosses the Maxwellian are tabulated below, together with the average moderator temperature during the experiment.

Series	Neutron Temp. $T_n(^{\circ}\text{C})$	D ₂ O Temp. $T_m(^{\circ}\text{C})$	Energy at which Maxwellian crosses dE/E (ev)
I	65 ± 10	31 ± 1	0.25
II	85 ± 10	33 ± 3	0.23
III	110 ± 20	36 ± 1	0.21

A discrepancy between experimental data and the sum of a Maxwellian distribution plus a dE/E distribution has been widely reported in the literature. Strictly speaking, there is no theory at present applicable to the spectra which have been measured in this experiment. The measurement was made of the energy spectrum leaking radially from the M.I.T.R. core tank, but the most nearly applicable theories are limited in derivation, if not in application, to infinite media - and more often to infinite homogeneous media.

Other experimenters have found that consideration of the effective absorption in finite media as $\Sigma_a + DB^2$ rather than

Σ_a brings the experimental results for neutron energy spectra in finite media into closer agreement with the theories developed for infinite media. To obtain a value of $\Sigma_a + DB^2$ for this experiment, a two group solution was used, giving

$$\Sigma_a + DB^2 = \frac{p \Sigma_{af} \phi_f}{\phi_{th}}$$

where Σ_a = thermal absorption cross section

D = diffusion coefficient

B^2 = buckling

p = resonance escape probability

Σ_{af} = slowing down cross section

ϕ_{th} = thermal group flux

ϕ_f = fast group flux

Charles Larson's thesis (Reference 4) gives a value for $\frac{\phi_f}{\phi_{th}}$ in the M.I.T. Reactor from a two group model which closely approximates the conditions of the experiment. Using this for the first series of experiments (i.e. no fuel in front of the 12-inch port) gives $\Sigma_a + DB^2 = 0.00603 \text{ cm}^{-1}$ as opposed to the Σ_a (of 99.6% D_2O) = 0.000121 cm^{-1} .

Using this value for effective absorption, an attempt was made to compare the experimental neutron current with the theoretical neutron flux. For the latter, simple slowing down, the Brown & St. John result (Reference 1), the heavy gas model (Reference 8) and the method of Coveyou, Bate and Osborn (Reference 2)

were used. The results of the comparison are given as Figure 7 A,B,C,D. The agreement is remarkably good, especially when it is recalled that the current and the flux are related by an energy dependent relationship of the form

$$J(E) = \text{const} \left[\phi(E,R) - \lambda_{tr}(E) \frac{\partial \phi(E,r)}{\partial r} \right]_R$$

where $J(E)$ = neutron current in the r direction

r = radius

λ_{tr} = transport cross section

$\partial/\partial r(\phi(E,r))$ and λ_{tr} are undetermined functions of energy.

The agreement of the data with the heavy gas model is very good. The curves of Brown & St. John and of Coveyou et al would be closer to the data if the presentation of their theoretical results (as a few widely spaced curves) permitted comparison.

To determine a theoretical neutron flux for the second and third series of experiments (i.e. with fuel in the region next to the 12-inch port) several approximations were made, the most important of which were that the change in Σ_a far outweighs the change in DB^2 , and that the Σ_a is the same as the Σ_a of the core. This results in $\Sigma_a + DB^2 = 0.01466 \text{ cm}^{-1}$ (for the present, no distinction is made between series II and series III). Because it is more amenable to calculation, the heavy gas model is compared to the data for series II & III (Figure 8). Again the agreement is good. For series II the calculated Σ_a is probably too high (being based on a regular array of fuel elements rather than just one element) and the DB^2 too low, while for series III the Σ_a is about right but DB^2 too low. The discrepancy between data and theory seems to agree with this.

5. Conclusion

Apparatus has been designed and built which is suitable for measurement of neutron energy spectra to a high degree of accuracy. Using this apparatus the energy spectrum of neutrons leaking from the M.I.T. reactor has been measured with several different fuel configurations. Although there is no reason to

expect good agreement between existing theory and these experiments, such agreement appears to exist when a simple correction is made to account for neutron leakage.

B. Semiconductor Neutron Spectrometer

1. General (G. Kaiz)

In the past several years semiconductor devices have been developed which are extremely good at detecting heavy charged particles. These devices are usually fairly small in sensitive area but are capable of energy resolutions of greater than 1%. An extensive survey of their characteristics can be found in Volume NS-8, January, 1961 of the IRE Transactions on Nuclear Science.

One of the applications described in the above reference is the use of these devices for neutron spectroscopy. This is done by putting a thin coating of a material like Li^6 between two of these detectors. Since Li^6 has a fairly large cross section for the $(n\alpha)$ reaction one uses the semiconductors to detect the α and triton emitted when the neutron is captured. By carefully measuring the total energy of these two particles it is possible to deduce the energy of the incident neutron. Since the two particles will come off nearly back to back one can reduce some of the background by only counting when there are coincident counts in the two detectors.

It was decided to try to develop a neutron detector of this type to determine the spectrum from the M.I.T.R. at energies higher than those obtainable by the chopper. These measurements would be carried out in the same port and under the same conditions as the chopper measurements.

2. Construction

The semiconductors used in this instrument have been obtained from Dr. H. W. Kraner of the M.I.T. Physics Department. He also was of great assistance in getting Li^6 films evaporated onto the detector. The detectors are all of the silicon-gold barrier type. Each detector is a square of $.25 \text{ cm}^2$ area and 1 mm

thick. They are mounted on fluorocarbon plastic to eliminate knock-on protons which create background problems when ordinary plastics are used.

In order to make the neutron detector, one of the pair of detectors to be used has a thin film of Li^6F evaporated onto it. The thickness is such that an incident light beam is reduced by 25% when passing through it. It was found this corresponds to a thickness of $150 \mu\text{g}/\text{cm}^2$. The two detectors are then placed facing each other with a very narrow gap ($\sim 0.010''$) between them to reduce the chance of a charged particle escaping. A diagram of the final detector is shown in Figure 9. The electronic hookup of the detector is shown in Figure 10.

The individual detectors have been checked with α ray sources and found to give a satisfactory response. The neutron detector is currently undergoing calibration checks prior to being placed into the reactor port.

C. Slow chopper

Design studies for a slow chopper have been started. This would be used to carry out spectral measurements below the fast chopper cutoff.

CHAPTER II

A. Investigations of Prompt Capture γ Ray Spectra

1. General

Ordinary activation analysis does not work for all elements because after capturing a neutron some species are stable or have a half life too short to be measureable. Since all elements emit prompt gamma rays when a neutron is captured, it was decided to investigate the possibility of doing neutron activation analysis using these prompt γ rays to identify the various elements. The principal difficulty with this method is that the γ rays to be measured vary in energy from about 1-9Mev. It is difficult to measure and identify the energy of these γ rays by ordinary NaI γ ray spectroscopy. The reason for this is that at these higher energies there is almost no photoelectric absorption of the γ ray, the Compton and pair production processes dominating. This means that very few of the γ rays actually give up their entire energy to the crystal. In fact the response to a monoenergetic γ ray at energies above about 2 Mev contains 3 peaks which may be of about equal magnitude. These arise from pair production interactions in which either none, one, or two of the annihilation quanta escape from the detector. Since capture γ ray spectra usually contain a number of γ rays with energies above 2 Mev this response makes determination of γ ray energies extremely difficult and in many cases impossible.

To solve this difficulty we have had designed and built a triple coincidence pair spectrometer. The principle is not new but the actual design should give considerably higher efficiency than other spectrometers of this type now in operation. In addition to the pair spectrometer we also have a bent quartz crystal spectrometer available for measuring energies less than 2 Mev. This spectrometer is described in reference 3 and was built under a National Science Foundation grant.

2. Triple Coincidence NaI Pair Spectrometer

(T. Hyodo, N. C. Paik)

a. Theory of Operation. The pair spectrometer consists of three NaI crystals. One is $1\frac{3}{4}$ " in diameter and 2" long, the other two are 6" in diameter and 3" long. These two large crystals have semi-cylindrical depressions in their ends so that when placed face to face there is a hole formed big enough to insert the $1\frac{3}{4}$ " crystal between them, see Figure 11.

In operation the collimated beam of γ rays to be measured impinge upon the small crystal. In some cases pair production will occur and the positron will be stopped and annihilated in the small crystal. The annihilation radiation will be emitted back to back and hence one will go in the direction of each of the bigger crystals. There is a good chance that each will escape from the small crystal and be detected in the large crystals. Thus if each of the large crystals simultaneously detects a 0.51 Mev quanta and these events are also in coincidence with a pulse from the small crystal, we know a pair production interaction has taken place in the small crystal and that the energy given up to it has been $h\nu - 1.02$ Mev.

In actual operation the circuit is hooked up as shown in Figure 12. All three crystals are in fast (~ 0.15 μ sec) coincidence. The signals from the large crystals are also fed through single channel analyzers which are set to pass 0.51 Mev pulses. The output of these analyzers and the fast coincidence are then put in slow coincidence (~ 6 μ sec). The output of the slow coincidence is then used to gate the 256 channel analyzer on so that it can analyze the pulse from the small crystal.

In addition to the above method of operation, it is also possible by changing a few connections to operate the system using the sum peak technique. The hook-up for this mode of operation is shown in Figure 13. The method of operation is useful when there are two or more γ rays in cascade. The sum of the preamplifier outputs is fed into one of the single channel analyzers which is set to the total energy of the cascade. The output of this analyzer is then used to gate the 256 channel analyzer on, and it analyzes the signal from one of the crystals.

Since all the energy of the γ transitions must be detected before the gating conditions are satisfied, the resultant spectrum shows only photopeaks and no Compton distribution. In this method the two crystals must be shielded from each other so that Compton scattered photons from one crystal are not detected in the other.

b. Description. Figure 14 shows the arrangement of the shielding. The coffin like shield consists of 5" of steel plus $3/4$ " of lead. The crystals, photo-multiplier tubes and preamps are located inside the shield. There is space available so that the two large crystals can be separated by as much as one foot if desired. This is particularly useful in the sum peak mode of operation. Access ports are available in the top, sides and bottom. In the pair spectrometer mode of operation the third crystal is inserted through one side port and the beam enters through the opposing side port.

This instrument was designed and built by the Atomium Corporation of Waltham, Massachusetts to specification supplied by M.I.T.

c. Performance. The instrument was received in late September so only preliminary performance tests have thus far been performed. Spectra of Na^{24} have been measured in the pair spectrometer mode of operation. The results are shown in Figure 15. The two peaks noted are the result of the two Na^{24} γ rays, the 1.38 Mev γ gives a peak at 0.36 and the 2.8 Mev γ gives a peak at 1.8. Note that all other types of interaction have been successfully rejected by the gating system. The Co^{60} spectrum has been observed in the sum peak mode of operation and is shown in Figure 16. Note that the entire Compton spectrum has been successfully rejected by the gating system. It is apparent from these results that the system will operate as intended.

It is now intended to use the system in conjunction with the reactor to look at prompt capture γ rays. The method for holding the sample under bombardment has already been designed and constructed. It is shown in Figure 17. This block of masonite with the sample inserted into it will be placed in front

of a reactor port. The γ rays from the sample will be observed with the pair spectrometer through the port at right angles to the incident neutron beam. This entire system is now ready for installation into the reactor.

d. Future studies. This instrument is now ready to be placed in operation at the reactor. The experiments planned are a series of measurements to determine the overall efficiency as a function of energy. This will be done by observing a series of samples that give off two or more γ rays of different energies and known relative intensities. The samples are chosen to cover the energy range from about 1 to 9 Mev.

After the calibration work is done, a number of samples will be carefully examined. The first will be germanium. It is hoped to determine how well the impurity content can be determined from changes in prompt γ ray spectrum. Other electronic materials such as silicon and selenium will also be studied.

3. Bent Quartz Crystal Spectrometer (J. Neill, I. Rahman)

In order to carry out the above studies at lower energies (below 2 Mev) a 6 meter bent quartz crystal spectrograph presently available (reference 3) at the M.I.T. Reactor will be used. It will be used to observe samples placed in the thermal column of the reactor as shown in Figure 18.

Preliminary studies to check overall operation have been carried out using a Sc^{45} source. In these experiments 7 lines having energies ranging from 50 to 300 Kev have been found. Preliminary results for these energies are 296, 229, 228, 217, 148, 143, 52 Kev. More accurate results will be available when final analysis of the plates has been completed. As soon as measurements on the Sc^{45} source have been completed it will be replaced by a Ge source and the low energy portion of the Ge spectrum observed.

B. Prompt α Analysis for Boron (L. Clark)

In order to measure trace amounts of boron in semiconductor materials an investigation has been undertaken which will make use of the $\text{B}^{10} (n, \alpha) \text{Li}^7$ reaction. This method had been used previously (reference 7) to determine the isotopic abundance of boron by direct counting of the prompt α ray.

In this investigation it is proposed to use an infinitely thick layer of sample on the inside of a proportional flow counter. Since the entire counter wall is to be coated by the powdered sample in a layer thick enough to absorb any α 's from the materials of construction, the background counts due to chamber impurities will mostly be eliminated. The B^{10} in the sample will be the principal source of α 's from the walls. This counter would then be exposed to a highly thermalized neutron flux such as is available in the medical therapy facility at the M.I.T.R. By proper electronic biasing secondary electrons from γ ray interactions can be eliminated so that only α ray or Li^7 pulses would be recorded.

A preliminary model of the above counter has been constructed and tested in the standard graphite pile in the Department of Nuclear Engineering Reactor Physics Laboratory. An improved model of this counter for use in the reactor is now under construction and should be in operation shortly.

C. Irradiation Facilities (D. Schwartz)

In order to carry out a broad program of sample irradiations it has been necessary to design and construct equipment capable of inserting and removing samples while the reactor is at power at several of the reactor irradiation facilities. Three different facilities have been built or improved to meet the needs of this irradiation program. These include the ball sample changer for use in 4TH1 - a 4" horizontal through port, a vertical sample changer for use in 3GV5 - a 3" vertical port, and some modifications and improvements in the rabbit facilities which are necessary for short half life studies.

1. Pneumatic rabbits

a. General. In order to conduct activation analysis studies of short half lived isotopes it was necessary to remodel and calibrate part of the rabbit system in the MITR. A hot cell is being built and the rabbits have been modified to deliver the samples inside the hot cell. A system for remote disassembly of the rabbits has been designed and installed. The circuitry of

the rabbits has been changed to provide greater control over irradiation times.

For activation analysis work with short half-lived materials, there are two basic requirements as to the mode of irradiation. The pneumatic rabbit system must be used, so that samples are available for counting in a minimum period of time after irradiation. Further, counting is normally done in the container in which it is irradiated, since it is desired that separation chemistry be performed only when absolutely necessary. Therefore, the irradiation container must not become any more than slightly active during short irradiations. Polyethylene has proven to be the best material available so far, in that it can withstand the impact of rabbit insertion and ejection, suffers only slightly from radiation damage (essentially none for short irradiations) and becomes only slightly active.

The recent rise in M.I.T.R. power level from 1.0 to 1.8 MW, with the planned rise to 2 MW, has introduced graphite temperatures in the range of 130°C. Since this is above the melting point of polyethylene, the power rise means that it is no longer possible to use polyethylene rabbits or vials in the reactor under all conditions. Air circulation is possible with the rabbit system, however, and it has been shown that temperatures with air circulation are well below the polyethylene softening point.

b. Rabbit Configurations. A complete investigation has been made of the temperatures in one rabbit tube. To provide a positive grip on the polyethylene rabbit, a long $\frac{3}{4}$ " OD polyethylene tube was pinned to the end cap. A chromel-alumel thermocouple wire ran up inside the tubing and through a small hole in the end cap. Then it was wound through a small piece of poly vial to reduce the shock to the wire caused by insertion or ejection. The thermocouple junction was inserted between several layers of polyethylene so that it was in good contact with the rabbit wall. A magnesium rabbit was used to measure equilibrium temperatures that were above the melting point of polyethylene. Two thermocouples were used, one just slightly penetrating through the end

cap, measuring the air temperatures, and the other embedded in the wall.

The internal construction of the rabbit tubes consists of two concentric tubes, the inner one perforated to provide circulation, with the rabbit traveling only in the inner tube. Solenoid valves control the flow of air and vacuum to the inner and outer tubes. Three configurations of the solenoid valves were investigated. The only other possible configuration is that tending to remove the sample, and therefore of no interest in measuring temperatures.

In the first configuration, air was placed on the inner tube and vacuum on the outer, which is the normal condition for inserting a rabbit. This condition prevails for all irradiations done on the automatic timer, and for any others which do not require the standby condition. In the second, the solenoids were reset and switched to standby, putting vacuum on both inner and outer tubes. This is the condition when no samples are being run, and was the condition during long manually operated runs at 1 MW. There will be a certain amount of circulation through the reactor, depending upon the unavoidable leakage into the tubes.

In the third configuration, with the system on operate, all solenoid valves are closed. This is the condition one rabbit tube is in when the other tube from the same chemistry area is used. Here the air circulation past the rabbit depends upon relative leakage past the air and vacuum solenoid valves. Finally, the first configuration, with full air circulation, was repeated. This case, giving the lowest temperature, is of maximum interest for higher power work.

c. Rabbit Temperatures. The rabbit tubes extend at right angles to port 12SH1, in which the fast chopper is inserted, and terminate underneath this port. Thus the addition of fuel in front of the chopper also affects the rabbit fluxes and temperatures. The effects on the temperature of having no fuel, one or two elements in front of the chopper, for various solenoid configurations, are shown in Figure 19. This shows that at 1 MW the rabbit temperatures do not rise above the softening point of

polyethylene under any circumstances. The small temperature difference between the temperatures with air low and ambient, and the rapid rate of decrease of temperature when air flow is turned on indicate that under proper conditions, polyethylene rabbits can be used even at 5 MW.

Temperature measurements were repeated when the power level was raised to 1.8 MW. The temperature was not allowed to get above 100°C with the polyethylene rabbit. The results are shown in Figure 20. The curve shows that at this power level, air flow must be on at all times when a polyethylene rabbit is in the reactor. Testing at 1.8 MW was continued with the magnesium thermocouple rabbit. The equilibrium temperatures at 1.8 MW and 1.7 MW are shown in Figure 21. The rate of decrease in temperature when air starts flowing is compared for the polyethylene and the magnesium rabbits in Figure 22. The difference in rates is due to differences in thermal conductivity.

Since a failure of the pneumatic blower with a polyethylene rabbit in the reactor could result in melting of the rabbit, an emergency system for either ejecting the rabbit or providing interim cooling is necessary. The normal procedure when the blower fails would be to shut down the reactor until repairs had been made. That the temperatures in this case do not become excessive is seen from Figure 23. In the case where the reactor can not be shut down, such as during a run in the medical facility, cooling is provided by an emergency CO_2 tank. The CO_2 flow rate is not sufficient to eject the rabbit. An indication that temperatures may be reduced in this manner is shown in Figure 21. A more complete test, showing that 20-25 psi of CO_2 will stop the temperature rise at a value sufficiently low so that no melting occurs is shown in Figure 24.

d. Rabbit Fluxes. Neutron fluxes and cadmium ratios in the rabbit tubes were also investigated, both absolutely and as a function of fuel loading. The absolute activity of cobalt foils was determined with a sodium iodide crystal and with conventional

coincidence equipment. The results are reported by Ram (Reference 5) and show the absolute thermal flux values at 1 MW with no fuel in front of 12SH1, in 1PH1, 1PH2, 1PH3 and 1PH4 respectively, to be 3.89, 4.06, 3.91 and 3.98×10^{12} neutrons/cm²-sec, with a five percent accuracy. Cadmium ratios taken at the same time indicate for a copper cadmium ratio, 118.4 ± 5 ; for cobalt, 55.3 ± 2 ; and for gold 20.5 ± 2 .

To measure the flux as a function of fuel loading in front of 12SH1, bare and cadmium covered copper foils of 1 mil thickness were irradiated in 1PH2. The foils were counted in a standard geometry about four inches above a 3 x 3" NaI (Tl) crystal. They were allowed to cool long enough to insure the complete decay of short lived Cu⁶⁶ activity. Then they were counted at intervals of several hours until they decayed to a point where background was an appreciable correction. The spectrum was plotted and the area under the 0.51 MEV peak was determined. This peak was due primarily to annihilation radiation from the Cu⁶⁴. After correcting the data for any one foil to a standard counting interval, the area under the peak, proportional to the count rate, was plotted against the time after irradiation. The data was extrapolated back with the half life of Cu⁶⁴ to zero time. The data points fell on the line, indicating that the peak was decaying with a pure copper half life. The intercepts were then corrected to a standard foil weight and compared to obtain relative thermal fluxes and cadmium ratios.

A comparison was made of three ways to determine the area under the peak. In the first, the peak was approximated as a triangle. In the second, a normal distribution was fitted to the data. Finally, peak heights were used as an indication of area. The second method proved to be the most reliable and less time consuming than the first. The area under a normal distribution is given by the product of a constant, the maximum value and the half width. The maximum and half width were obtained experimentally, and since relative readings only were necessary, the constant was unimportant. The third method used

was an approximation to this, assuming a constant half width, which would be true were there no shift in the gain of the system.

The following thermal fluxes were obtained using Ram's value of $4.1 \pm 0.2 \times 10^{12}$ neutrons/cm²-sec for tube 1PH2 for Case I, with no fuel in front of 12SH1. For Case II, with a fuel element in position number 26, the flux was $3.8 \pm 0.2 \times 10^{12}$, and for Case III, with fuel in both positions number 25 and number 26, the flux was $4.3 \pm 0.2 \times 10^{12}$. The copper cadmium ratios using 7 mil copper foils were measured as 113 ± 7 for Case I, 46.7 ± 1.9 for Case II, and 45.7 ± 1.3 for Case III. It must be noted that fuel positions number 25 and number 26 are not symmetrical with respect to 1PH2, position number 26 being considerably closer to the end of the tube.

2. Vertical Facility

The Vertical Sample Changer facility is another means of inserting or removing samples from the reactor while the reactor is at power. Shielding is provided by raising and lowering the sample, encased in an aluminum can, through a serpentine tube in the lower shield plug (see Figure 25). The aluminum can uses a cover with a raised conical section, which can be gripped with a special handling tool using pneumatically operated gripping fingers.

The operation is as follows. The sample plug is removed and the shutter mechanism is rotated until the index mark indicates that the through hole is lined up. The sample can is lowered with the grapping tool until it is at the bottom of the tube, and the tool is released. The can is usually dropped slightly at the end of the tube, so that an audible indication that the can has been released is obtained. The tool is then brought out of the high flux region.

At the end of the irradiation the tool is again lowered until it rests on the can, and the fingers are made to grip the can. It is then drawn up above the shutter mechanism, and this is rotated until one of the storage holes is lined up. The can is then placed in the storage hole until the cooling period, to

allow for the decay of aluminum and other short half lived isotopes, is over. The can may then be removed from the shutter for further handling.

The insertion time of a sample can be as rapid as a few seconds. The facility has been used extensively for irradiations of from one minute to a day, provided that 30 to 45 minutes of cooling time may be allowed for adequate aluminum decay. Absolute flux measurements at 1 MW indicate a thermal flux of $5.0 \times 10^{12} \text{ n/cm}^2\text{-sec}$.

3. Ball Sample Changer

The Ball Sample Changer facility provides another means of inserting or removing samples from the reactor while at full power, without any radiation hazard. During irradiation, the sample is encased in an aluminum sample can which is placed into an aluminum ball. The ball is held in one of eight cups in the graphite carriage (see Figure 26).

The operation is as follows: The handwheel is rotated, moving the inner shield plug-graphite carriage assembly outward with respect to the outer shield plug. This is continued until index marks indicate that the proper graphite cup is directly under the inlet hole in the outer shield plug. The sample ball is then rolled by gravity down a tube from the reactor face to the inlet hole and into the cup. Rotating the handwheel then inserts the graphite carriage section into the reactor. All cups may be used simultaneously.

To remove the sample, the handwheel is rotated until the index mark indicates that the graphite cup is once more lined up with the inlet hole. The apparatus is left in this position during the cooling period, to allow for decay of aluminum and other short half lived isotopes. The entire inner shield plug-graphite carriage assembly is then rotated until the outlet hole is lined up, and the ball rolls by gravity down another tube from the outlet hole to the reactor face, where it emerges into a special lead pig. The ball is then disassembled with remote handling tools.

Since complete insertion takes several minutes, this facility is not good for short runs. However, it has been very useful for runs of a day or more. The maximum size of sample is about half that for the vertical facility. Preliminary calibration of the flux in the ball sample changer facility at 1 MW, using a sodium source in position number 5, indicated a thermal flux of $3.5 \times 10^{12} \text{ n/cm}^2\text{-sec}$. An absolute flux calibration with gold foils indicated a thermal flux of $3.75 \pm 0.2 \times 10^{12} \text{ n/cm}^2\text{-sec}$ in the same position. The flux falls off slightly on both sides of this central position.

D. Irradiations

In addition to the irradiations performed in conjunction with the work previously described, the M.I.T. Reactor has been used to irradiate samples for other groups at Air Force Cambridge Research Laboratories. Over the period covered by this report, a total of 86 irradiations have been performed in this manner, using seven different reactor facilities.

REFERENCES

1. Brown, H.D. and St. John, DP33 (1954).
2. Coveyou, R.R., R.R. Bate and R.K. Osborn, J. Nuc. En. 2, 153 (1956).
3. Kazi, A.H., N.C. Rasmussen and H. Mark, Rev. Sci. Instr. 31, 983 (1960).
4. Larson, C.L., Sc.D. thesis, M.I.T., Cambridge, Mass. (1959).
5. Ram, K.S., Course 22:42 Report, M.I.T., (1961).
6. Teich, M. and P. Schweitzer, B.S. thesis, M.I.T., Cambridge, Mass. (1961).
7. Wanke, H. and E.U. Mouse, Z. Naturforsch, 10a, 667 (1955).
8. Wilkins, J.E., CP-2481 (1944).

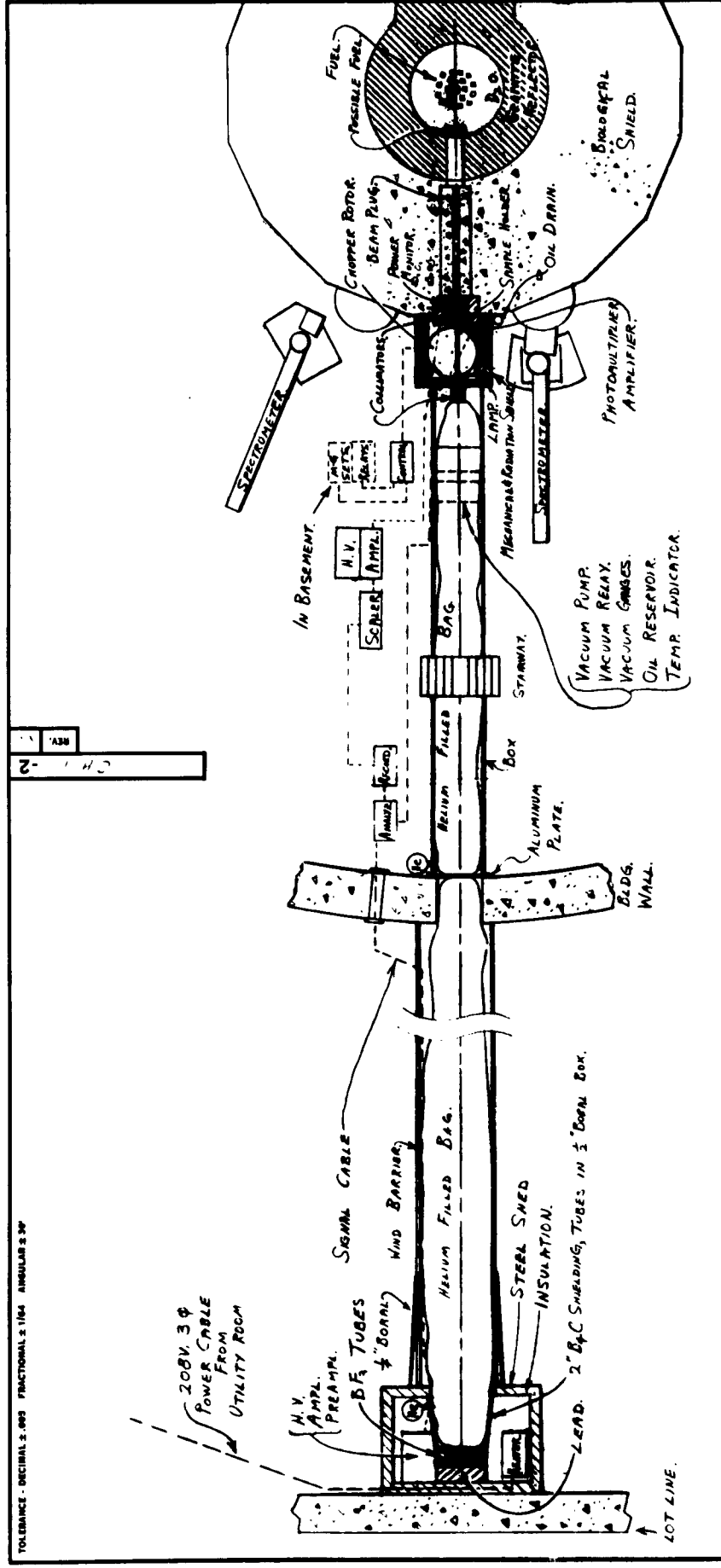


FIG. I SYSTEM LAYOUT

MASSACHUSETTS INSTITUTE OF TECHNOLOGY REACTOR	
MITR FAST CHOPPER	
SYSTEM SCHEMATIC	
DATE	9-15-57
DRAWN BY	C.A.A.
APPROVED	C.H.1
REV.	-2

MATERIAL	QUANTITY	SCALE
9-15-57	C.A.A.	C.H.1
DATE	DRAWN BY	APPROVED

REV.	DESCRIPTION	BY	DATE
A	COMPLETE REVISION	MA	F.20.51

TOLERANCE - DECIMAL ± .003 FRACTIONAL ± 1/64 ANGULAR ± 30°

RESOLUTION DETERMINED BY $\frac{\Delta E}{E} = -0.0279 \frac{\Delta \tau}{m} \sqrt{E + 2 \frac{\Delta m}{m}}$

— DUE TO $\Delta \tau$ OF ROTOR, ANALYZER, DETECTOR LENGTH, COLLECTION TIME

---- DUE TO $\Delta \tau$ OF ROTOR ALONE

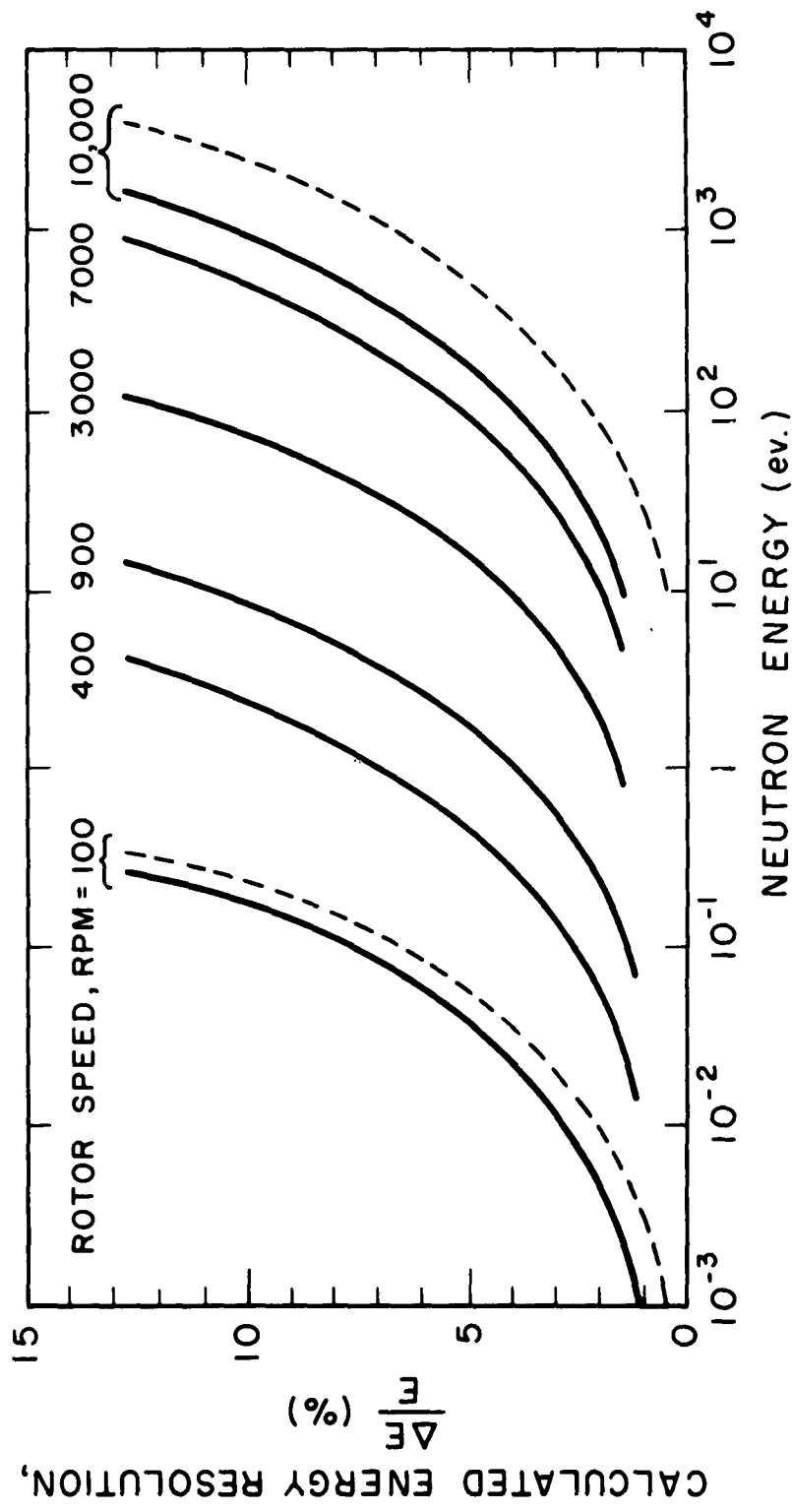


FIG. 2 ENERGY RESOLUTION

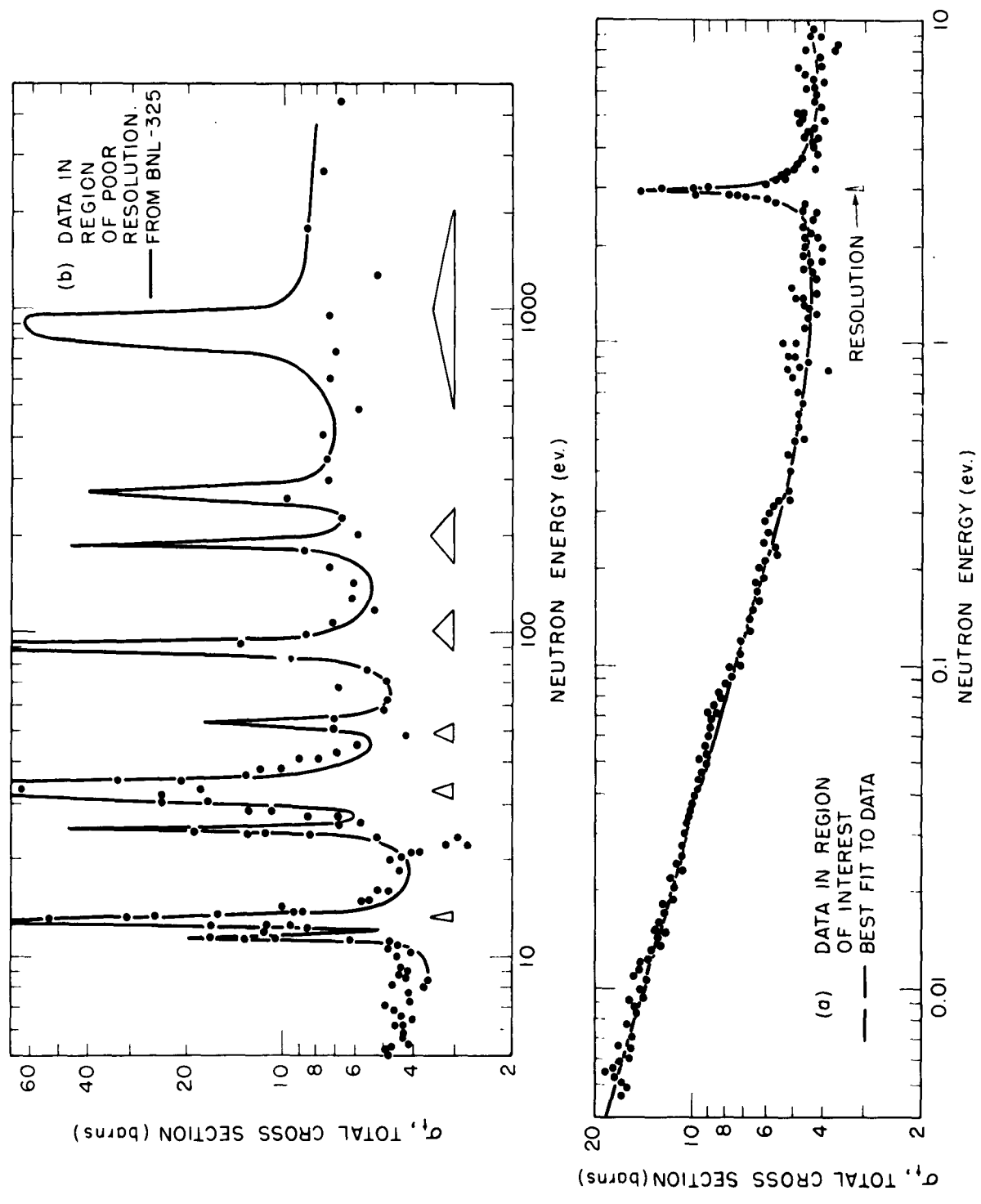


FIG. 3 TOTAL CROSS SECTION OF PALLADIUM

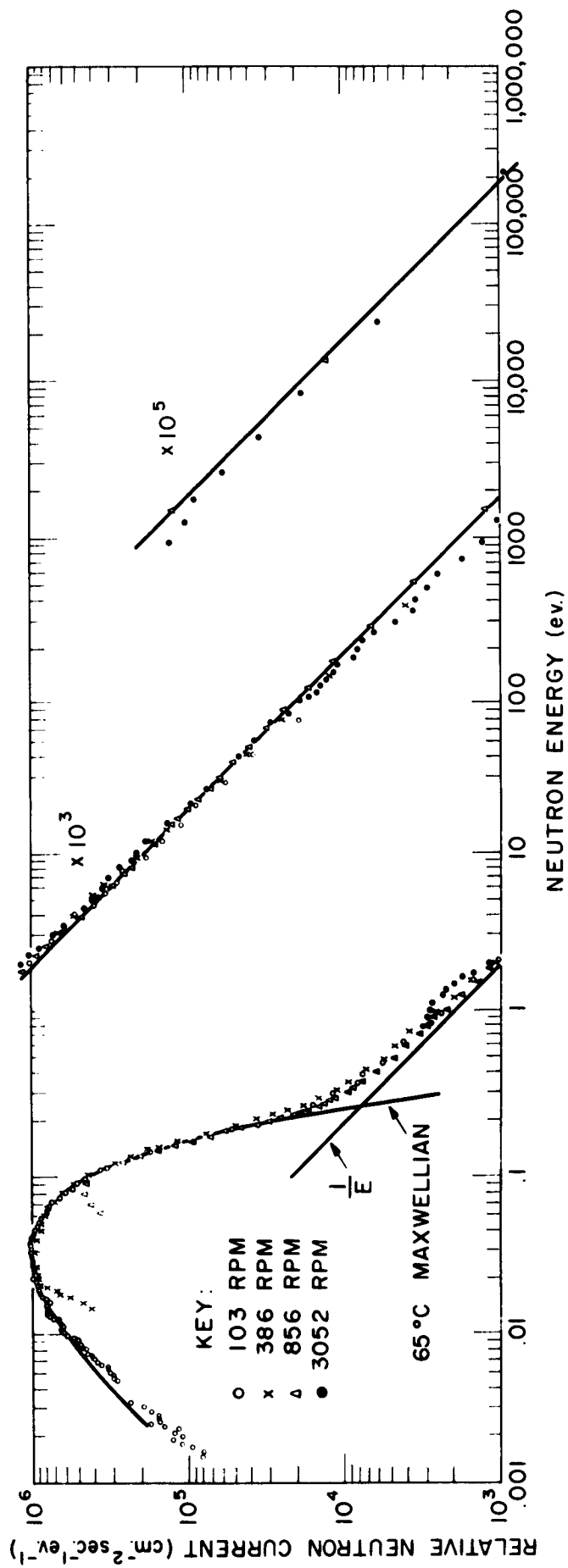


FIG. 4 LEAKAGE NEUTRON ENERGY SPECTRUM, FIRST SERIES OF EXPERIMENTS. NO FUEL IN FRONT OF 12 IN. PORT

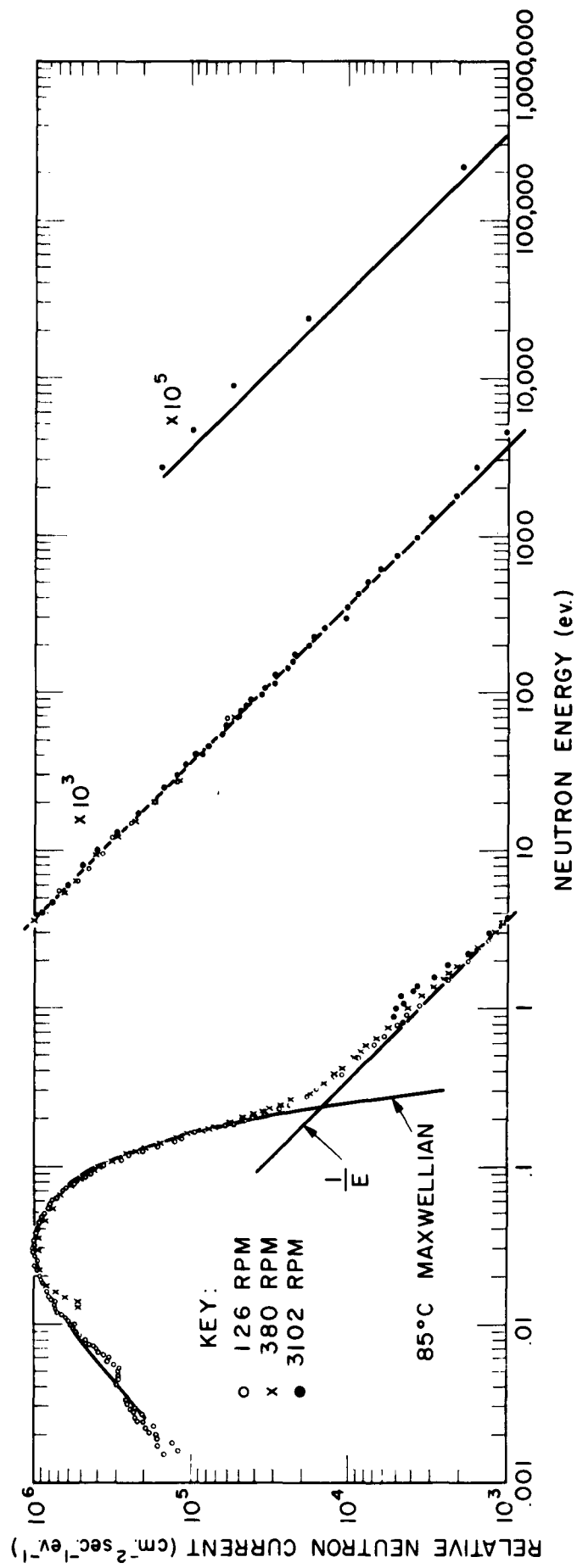


FIG. 5 LEAKAGE NEUTRON ENERGY SPECTRUM, SECOND SERIES OF EXPERIMENTS. ONE FUEL ELEMENT IN FRONT OF 12 IN. PORT

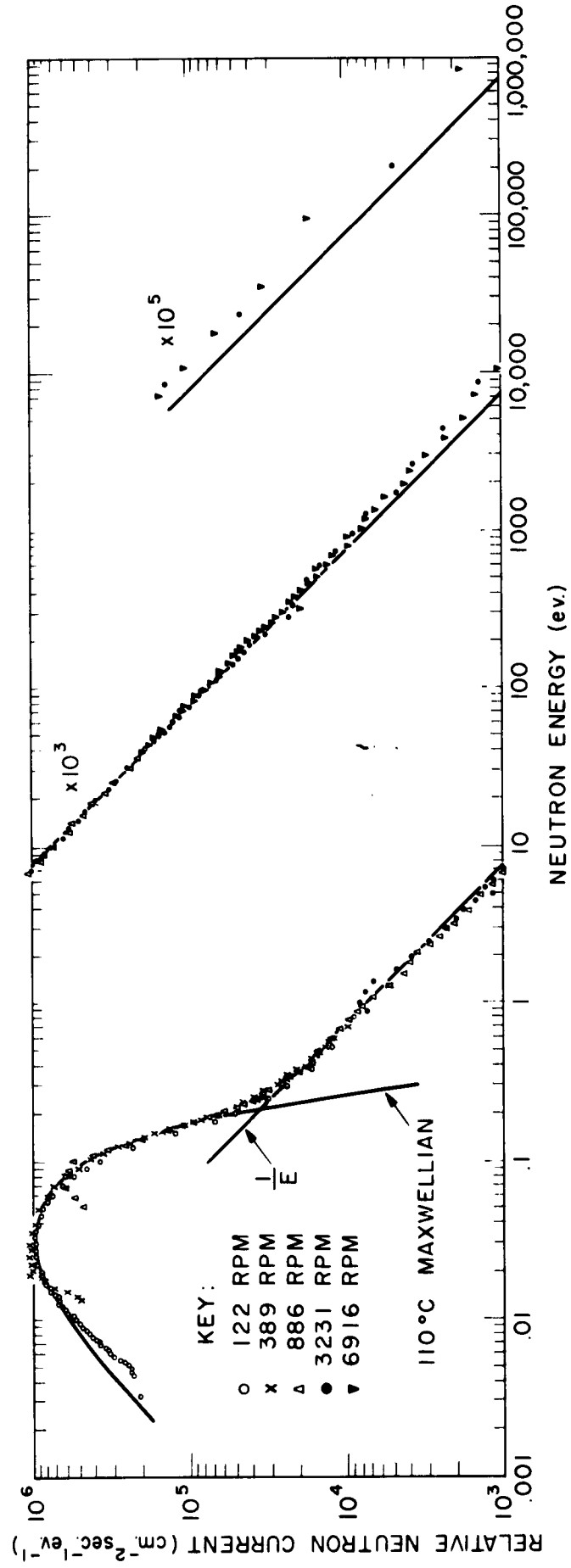


FIG. 6 LEAKAGE NEUTRON ENERGY SPECTRUM, THIRD SERIES OF EXPERIMENTS. TWO FUEL ELEMENTS IN FRONT OF 12 IN. PORT

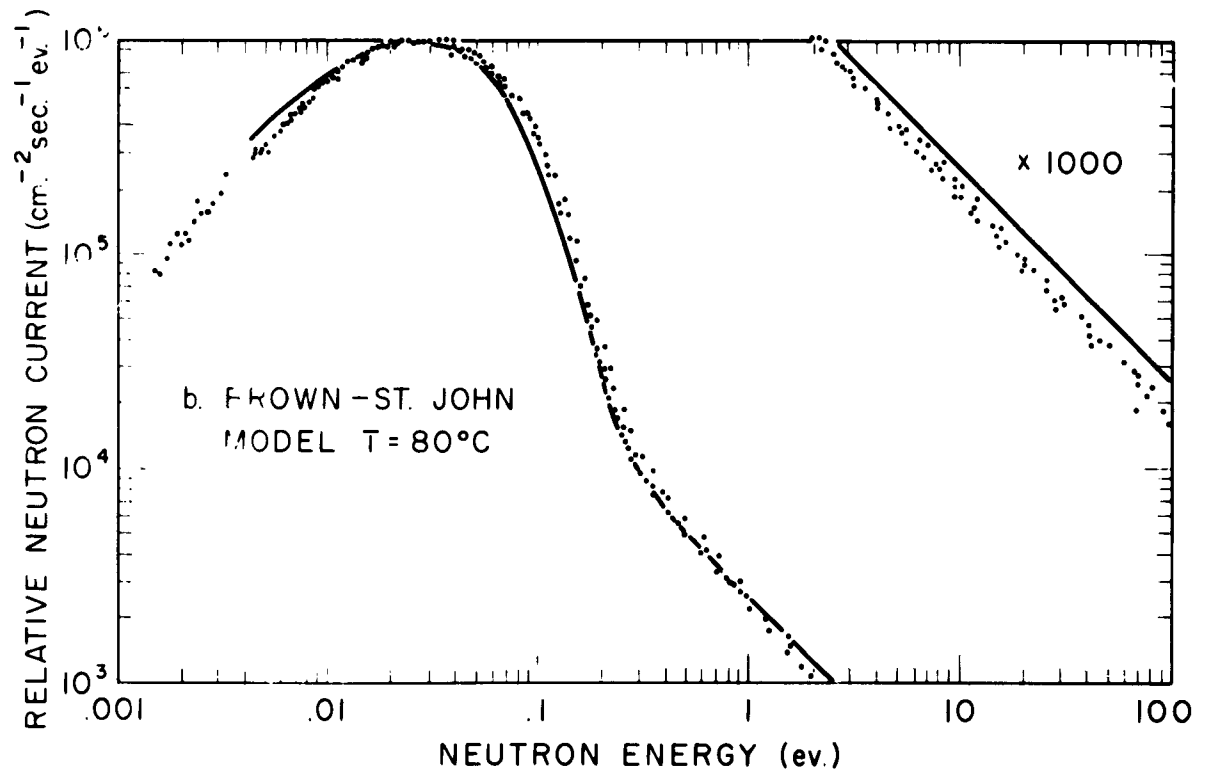
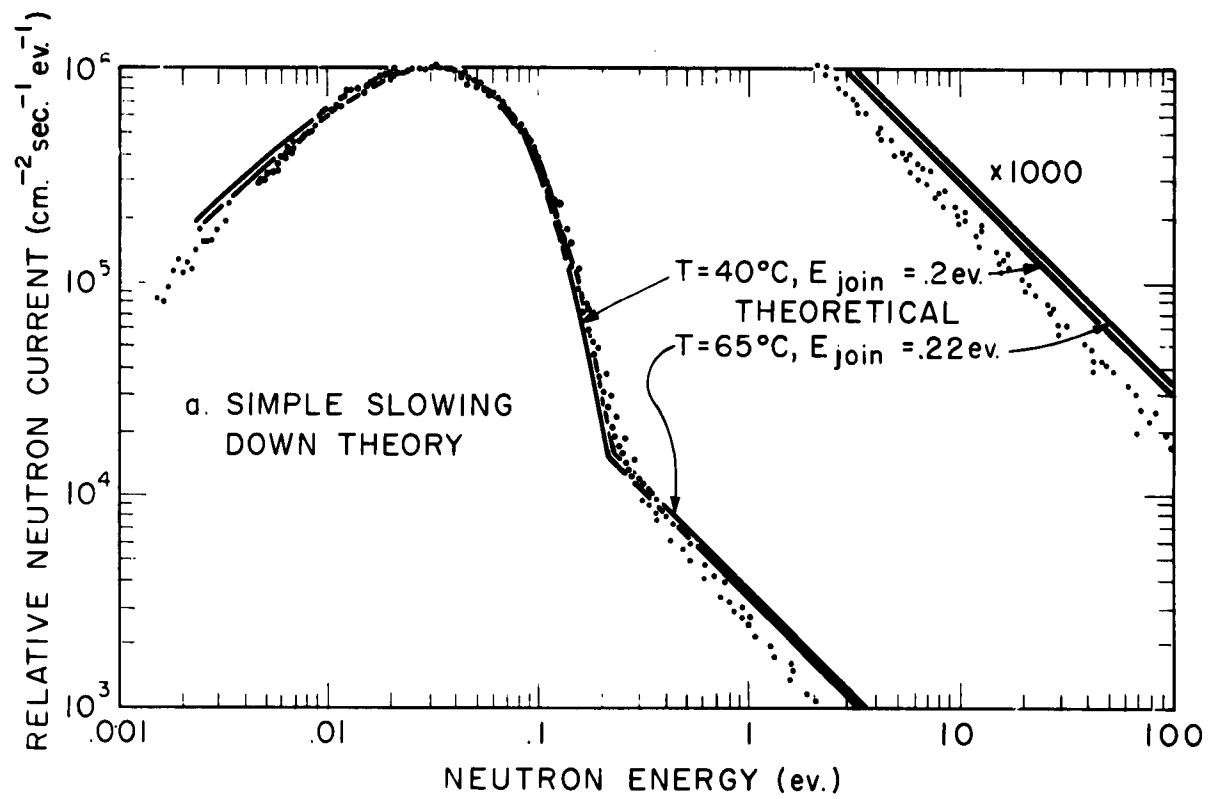


FIG. 7A, 7B EXPERIMENTAL NEUTRON CURRENT AND THEORETICAL FLUX. SERIES I. NO FUEL IN FRONT OF 12" PORT
CALCULATED $\Sigma_a + DB^2 = 0.00603 \text{ cm}^{-1}$

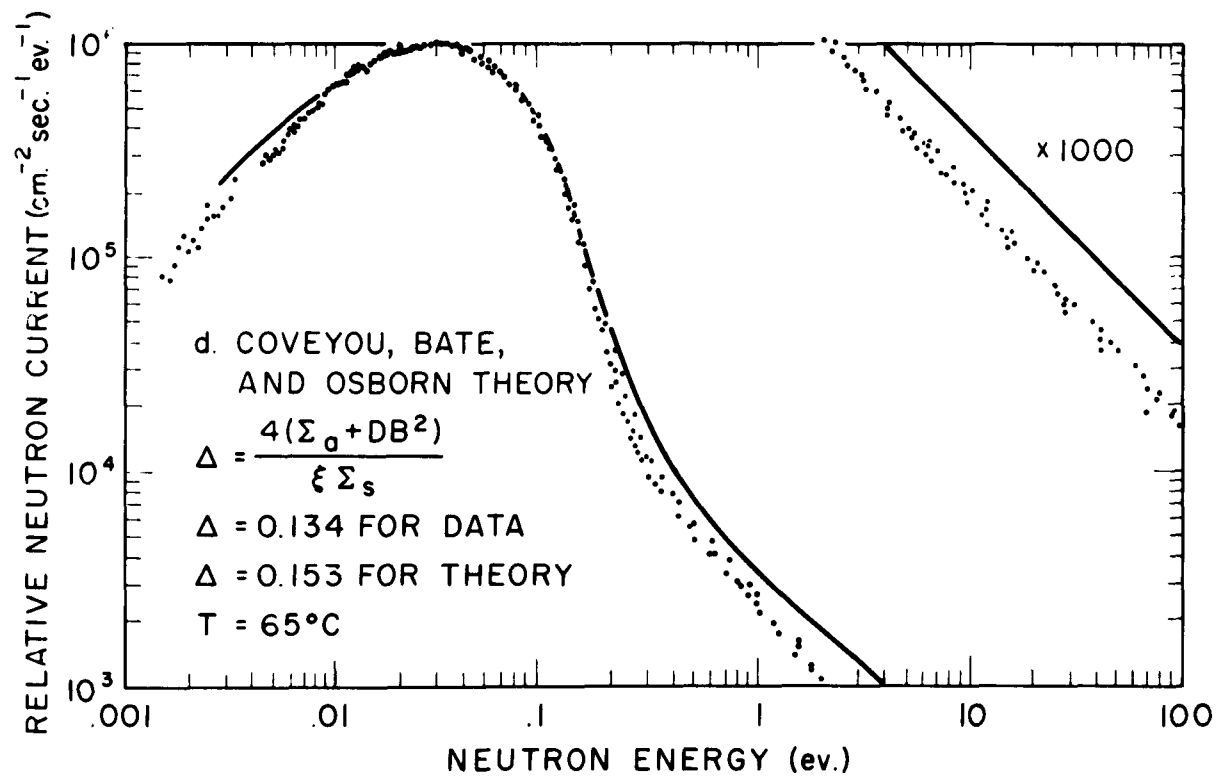
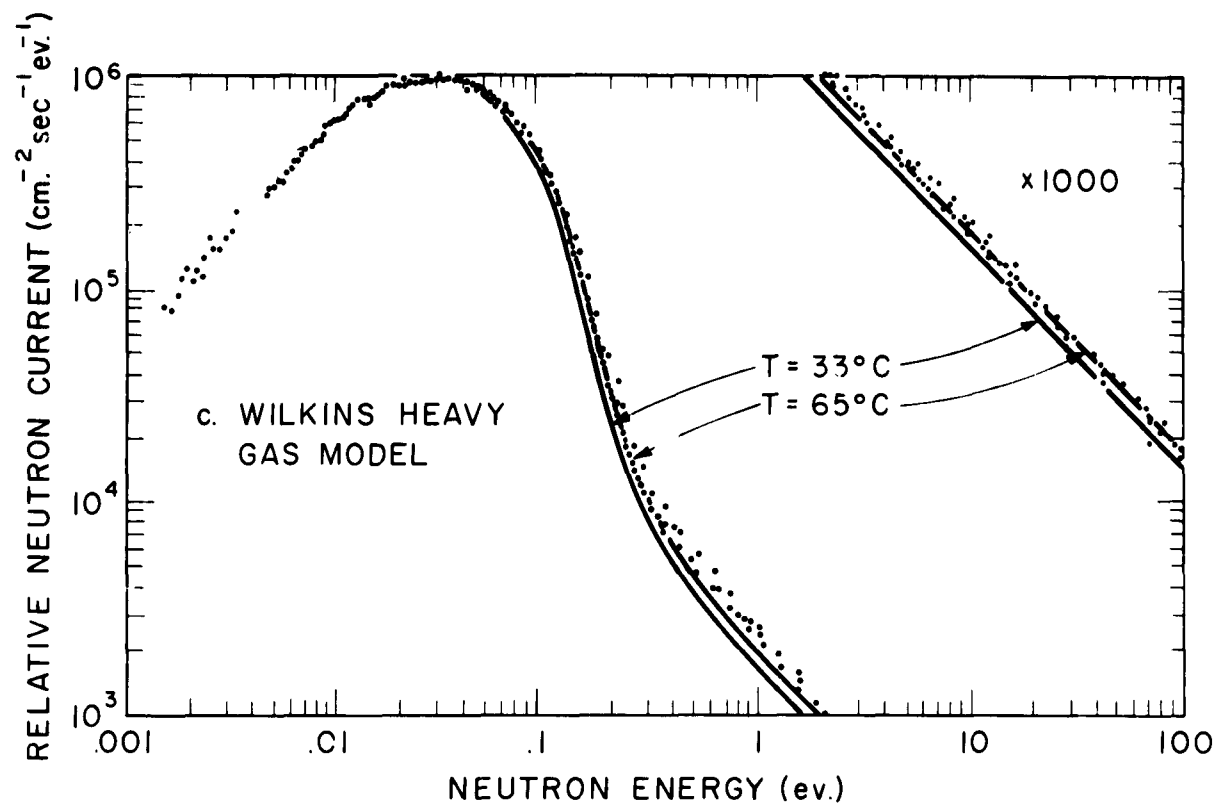


FIG. 7C, 7D EXPERIMENTAL NEUTRON CURRENT AND THEORETICAL FLUX. SERIES I. NO FUEL IN FRONT OF 12" PORT
 CALCULATED $\Sigma_0 + DB^2 = 0.00603 \text{ cm}^{-1}$

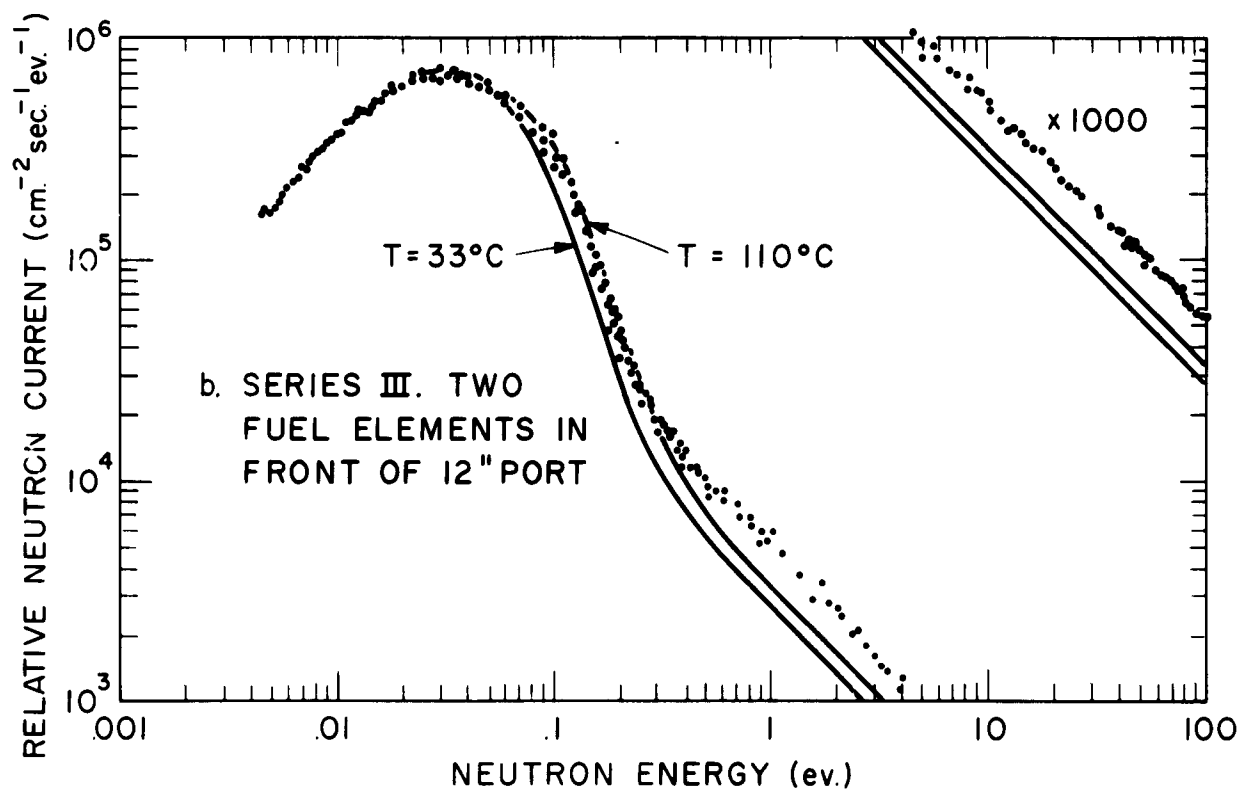
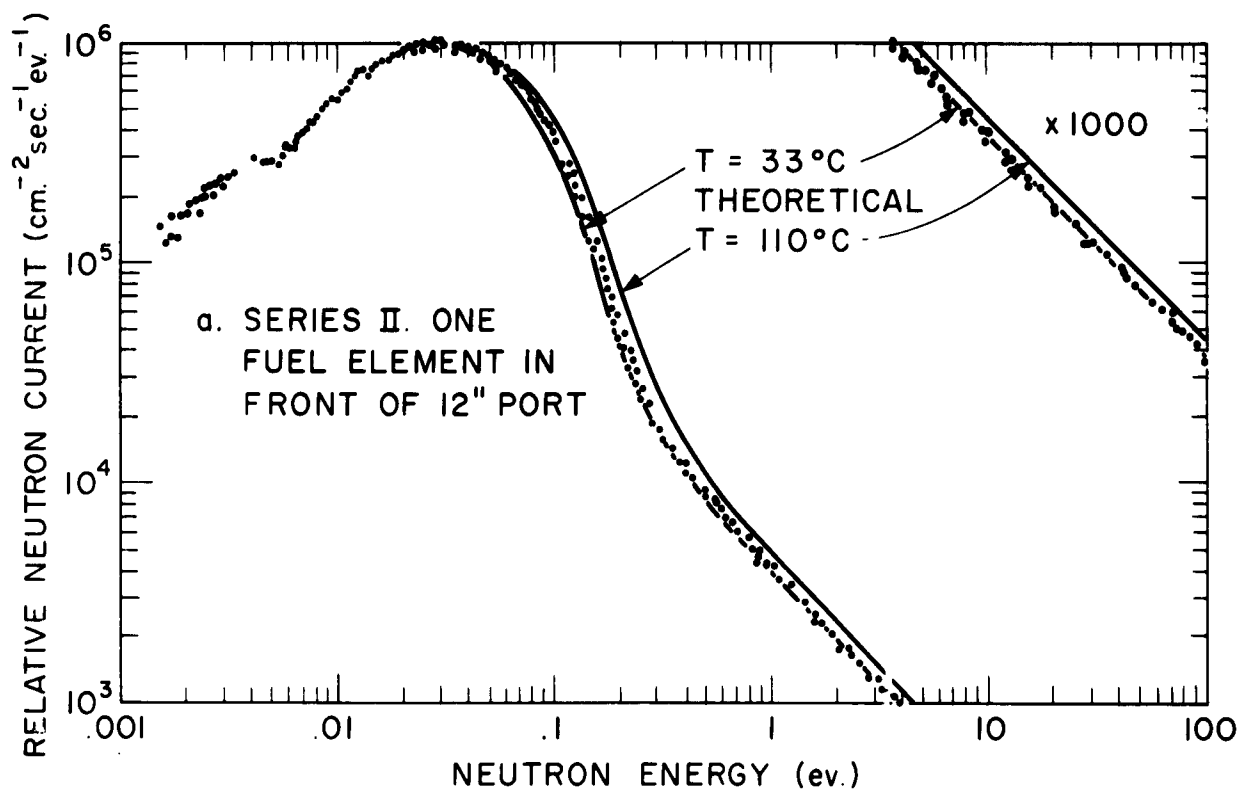


FIG. 8 EXPERIMENTAL NEUTRON CURRENT AND THEORETICAL FLUX FROM WILKINS HEAVY GAS MODEL.
CALCULATED $\Sigma_a + DB^2 = 0.01466 \text{ cm}^{-1}$

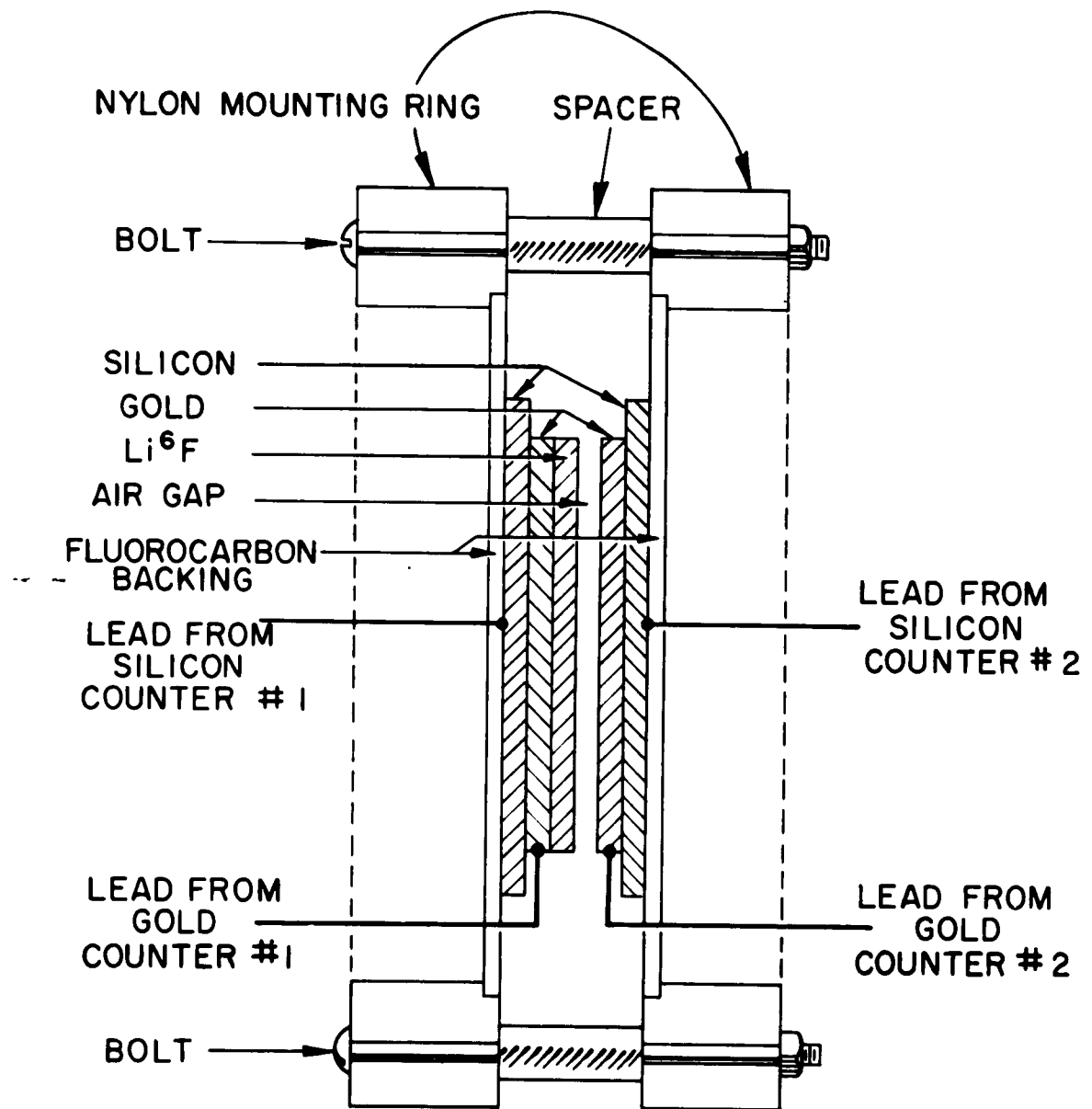


FIG. 9 NEUTRON COUNTER MOUNTING

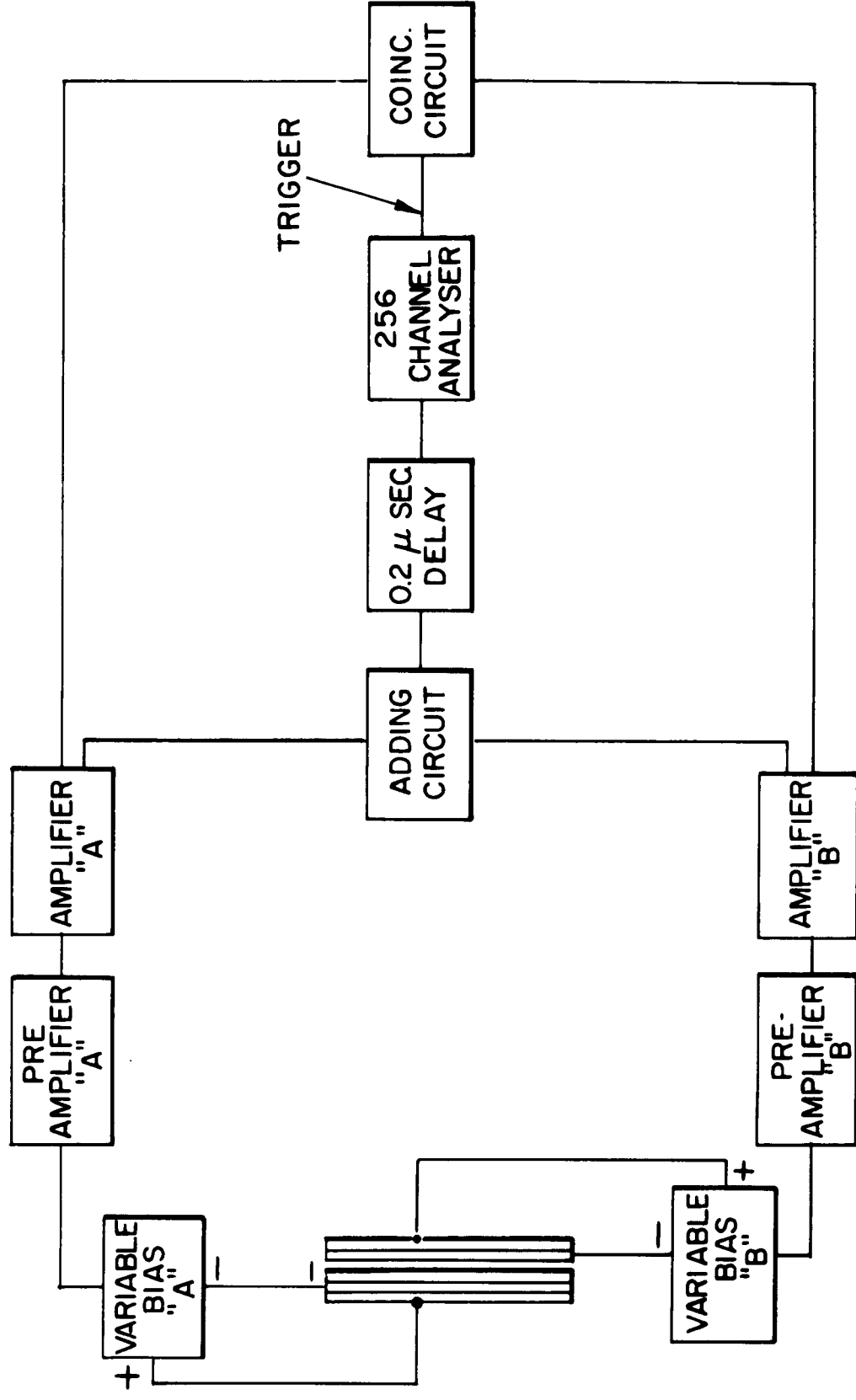


FIG. 10 ELECTRONICS FOR NEUTRON SPECTROMETER

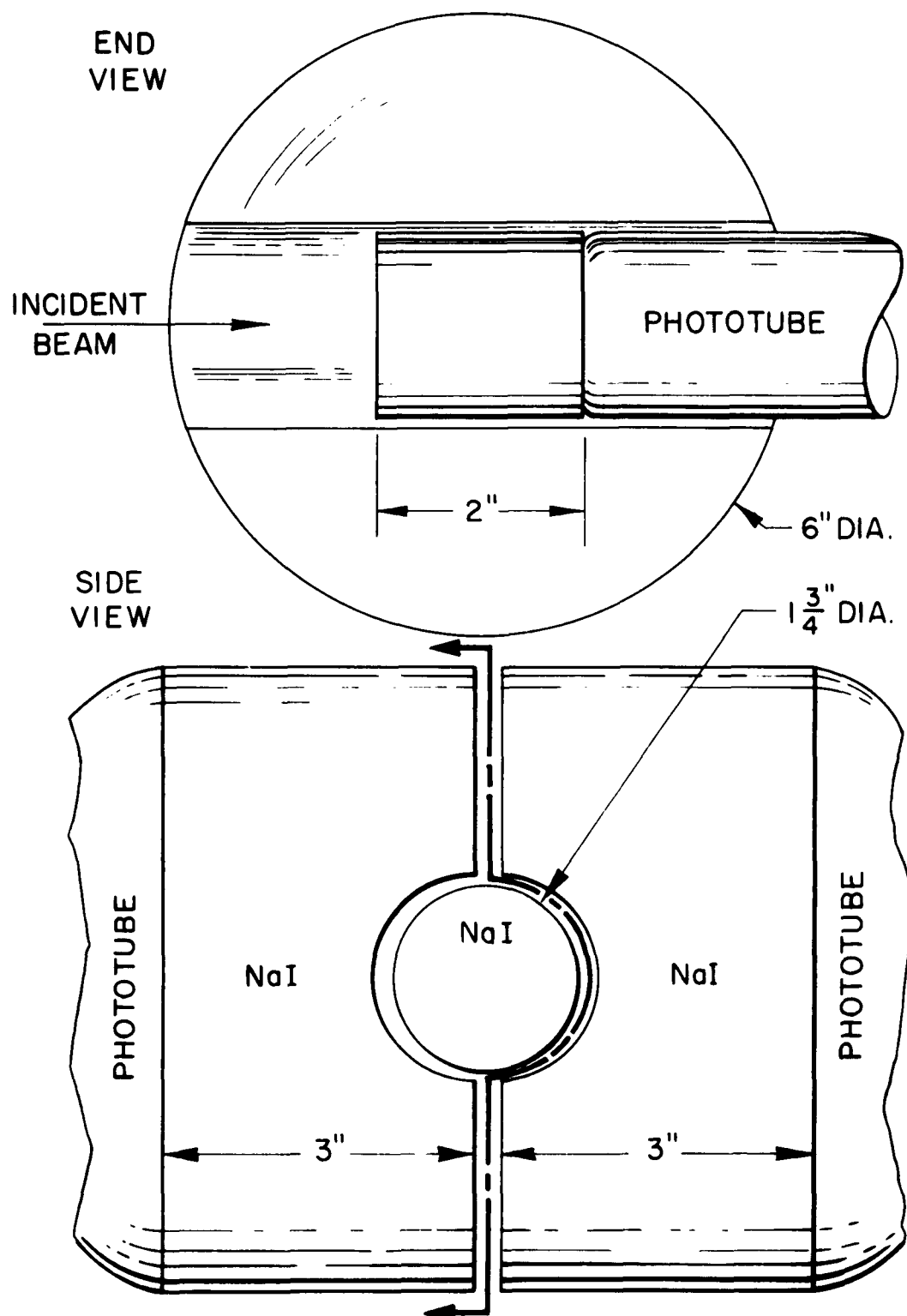


FIG. 11 ARRANGEMENT OF NaI CRYSTALS IN TRIPLE COINCIDENCE PAIR SPECTROMETER

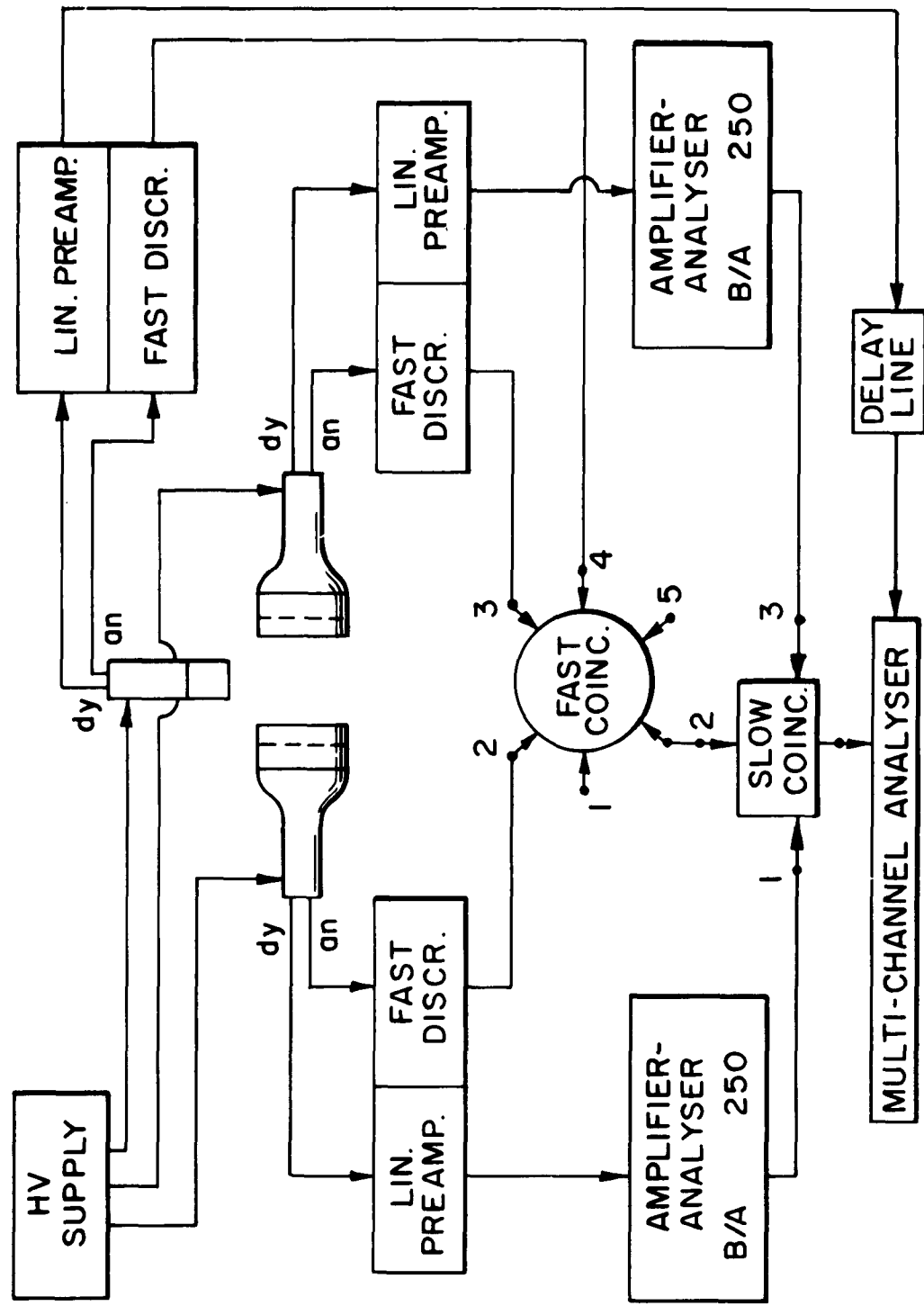


FIG. 12 BLOCK DIAGRAM OF TRIPLE COINCIDENCE UNIT

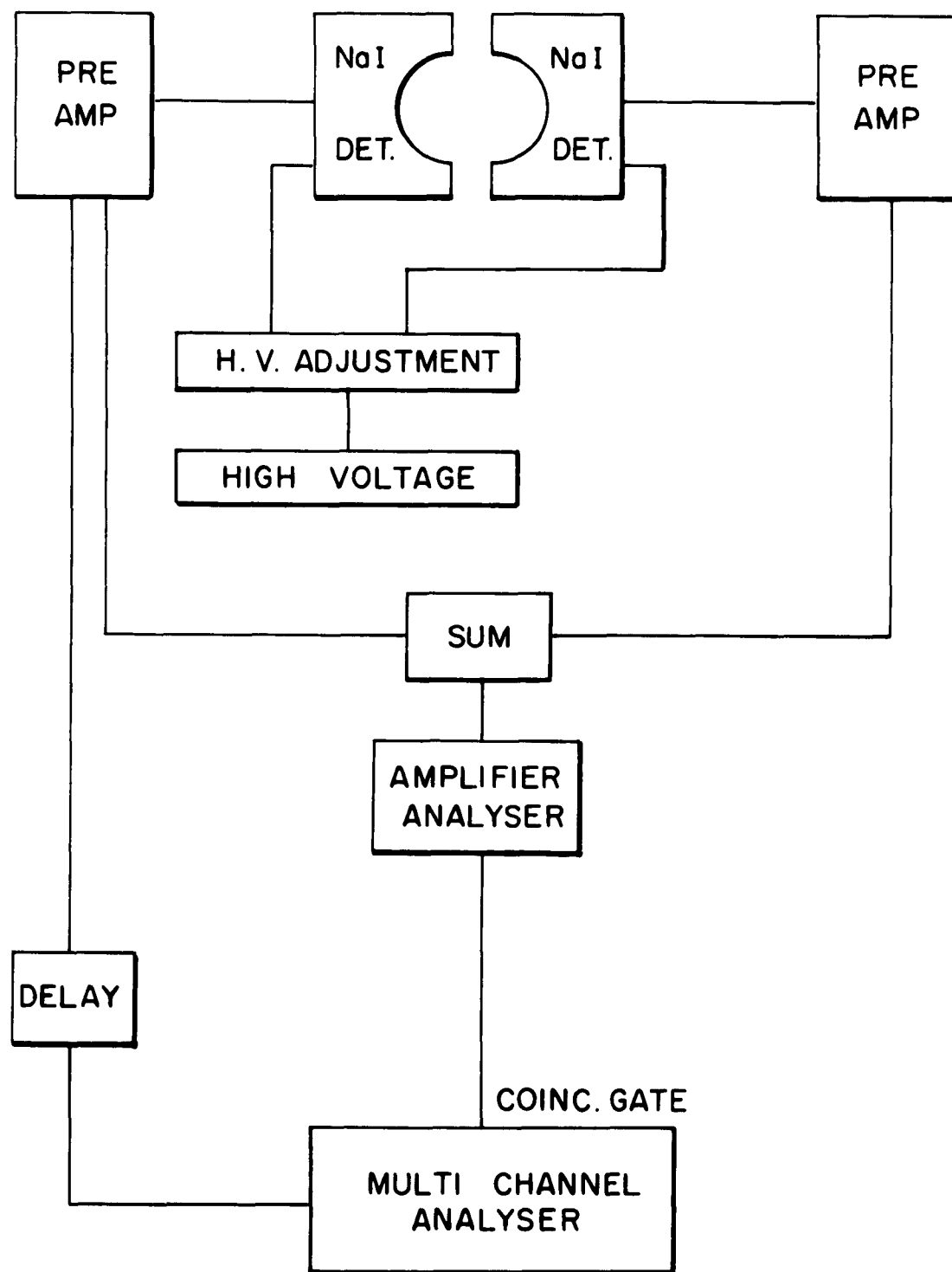


FIG.13 BLOCK DIAGRAM OF SUM PEAK CIRCUITRY

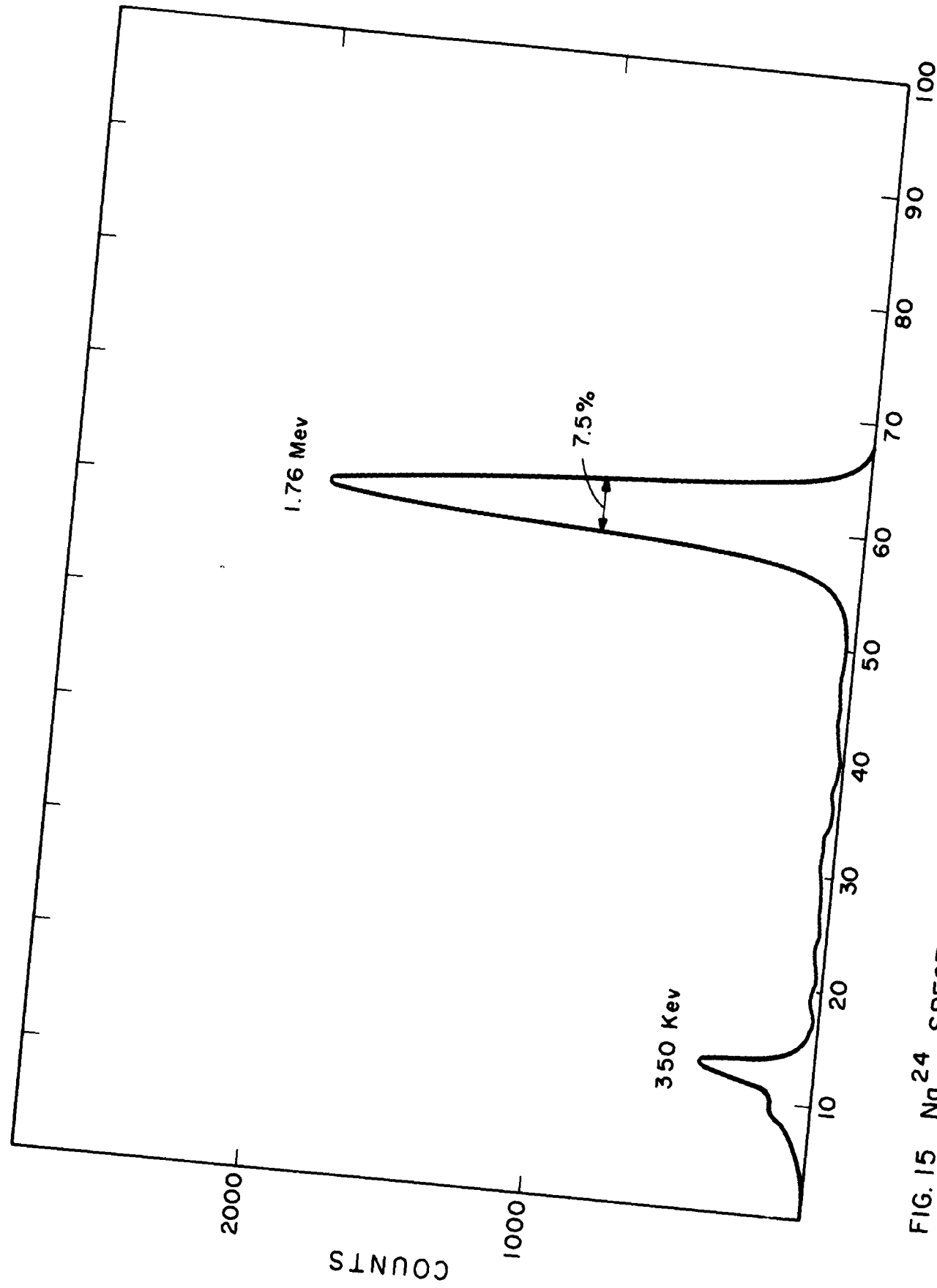


FIG. 15 Na^{24} SPECTRUM FROM TRIPLE COINCIDENCE PAIR SPECTROMETER

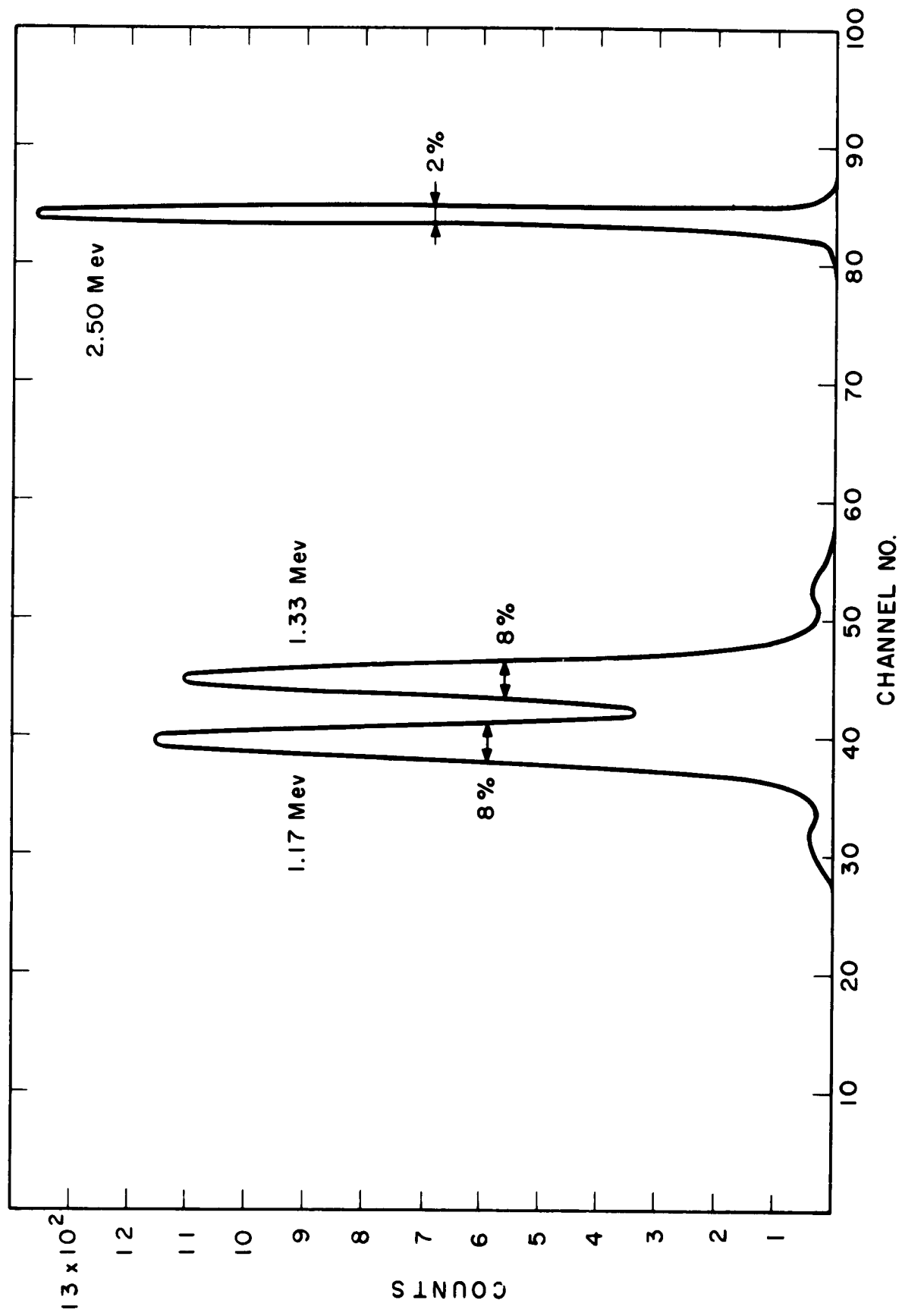
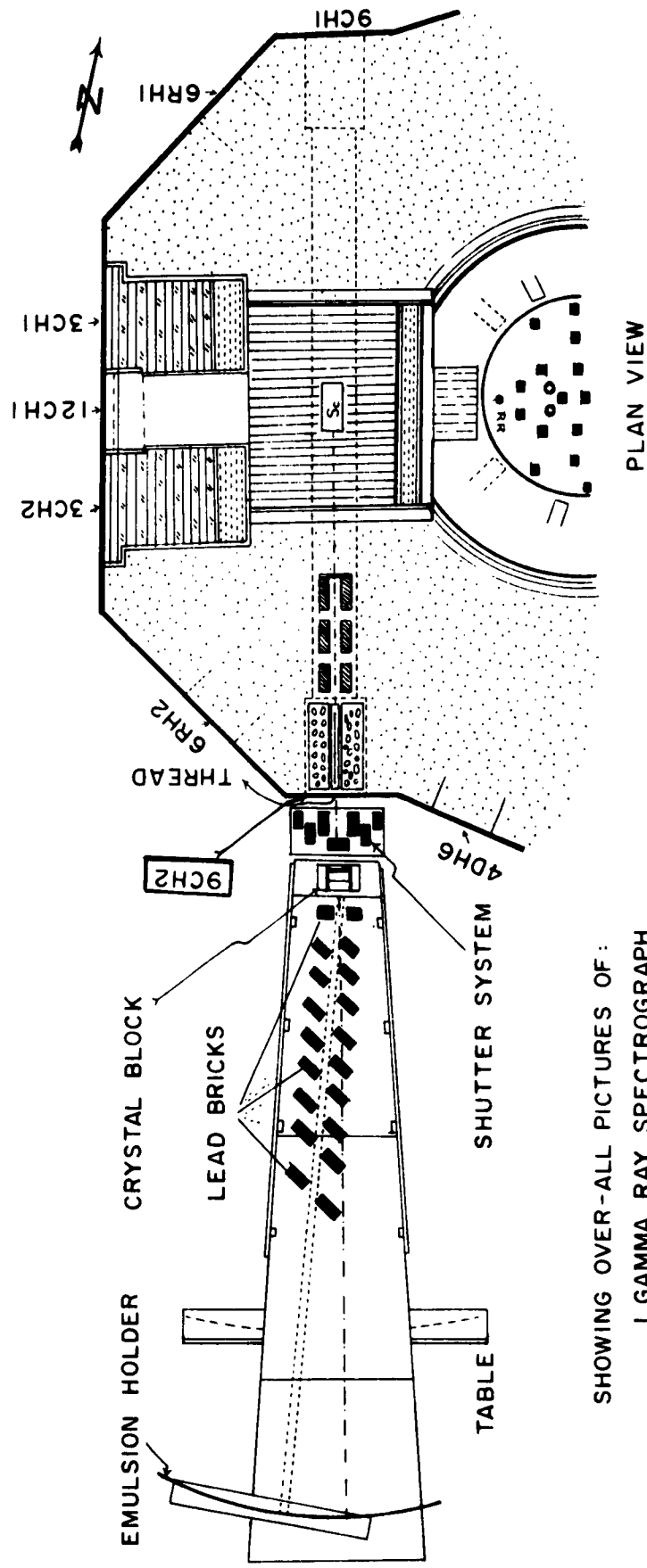


FIG.16 Co^{60} SPECTRUM (SUM PEAK METHOD)



SHOWING OVER-ALL PICTURES OF:

1. GAMMA RAY SPECTROGRAPH
2. CALIBRATION SOURCE & PLUG ASSEMBLY
3. MIT REACTOR CROSS-SECTION SHOWING SCANDIUM SOURCE & COLLIMATING BRICKS IN 9CH2 PORT
4. SHUTTER SYSTEM

FIGURE 18

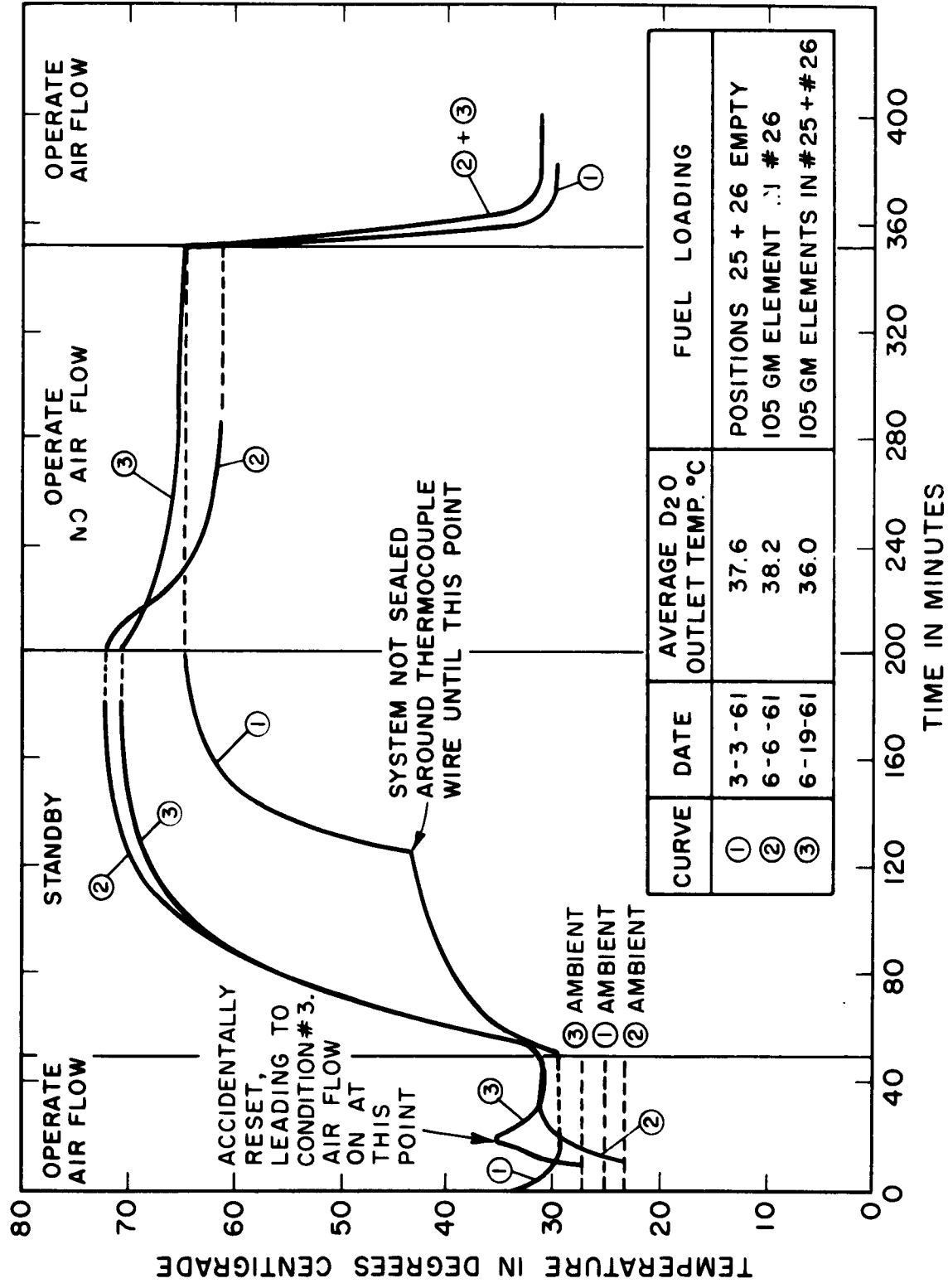


FIG. 19 TEMPERATURE IN RABBIT TUBE IPH4 AS A FUNCTION OF FUEL LOADING

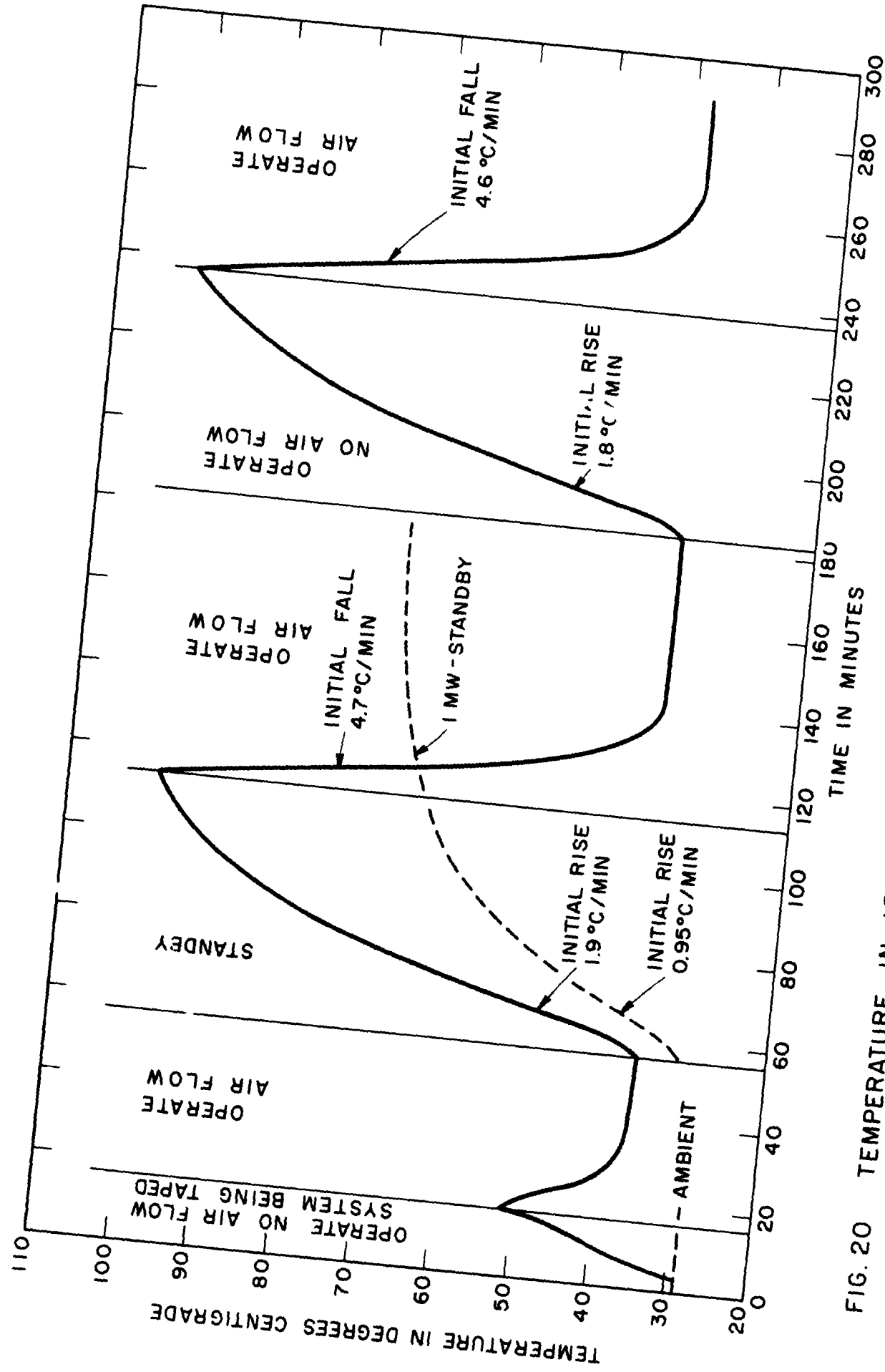


FIG. 20 TEMPERATURE IN IPH4 AT 1.8 MW

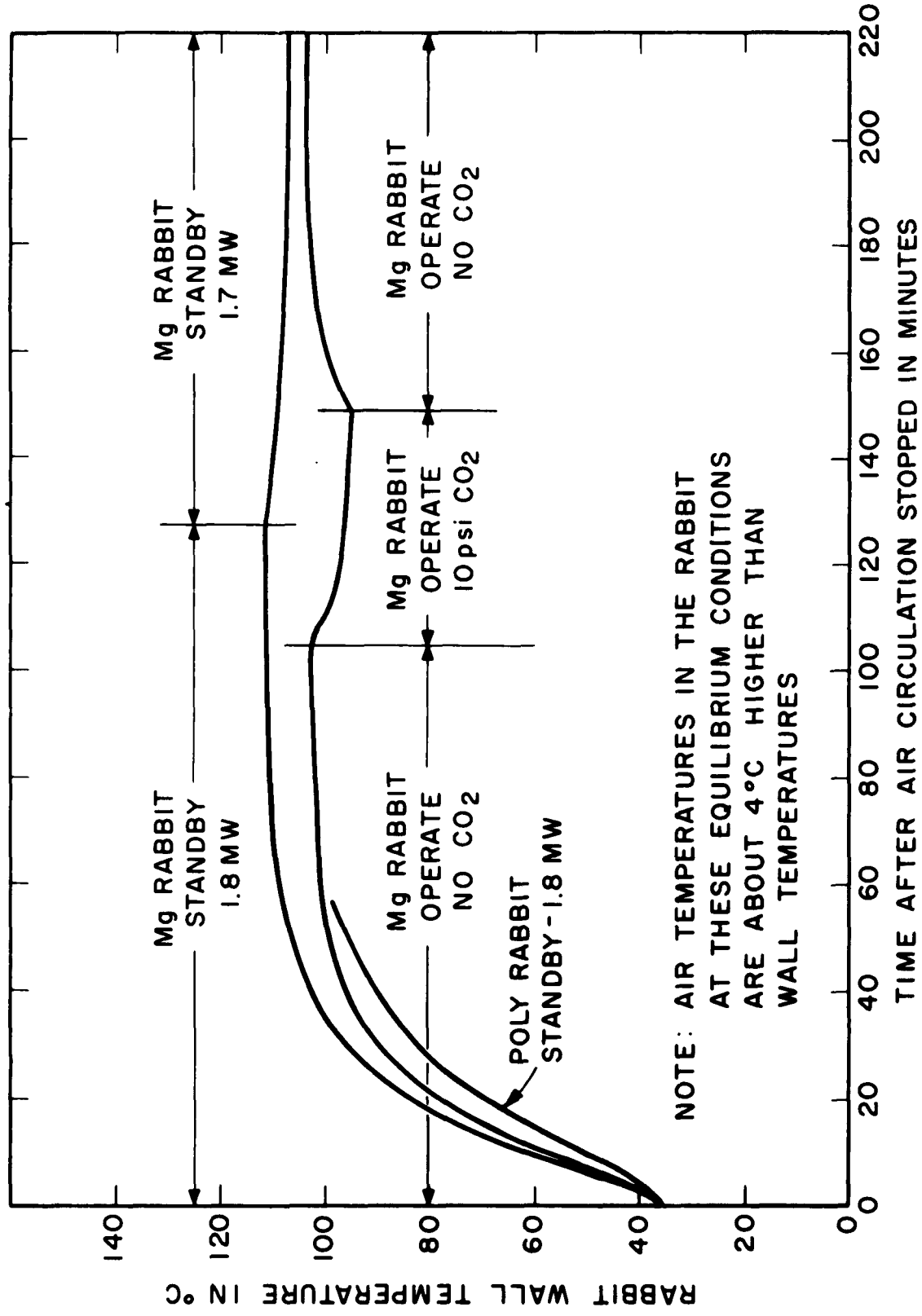


FIG. 21 RABBIT EQUILIBRIUM TEMPERATURES AS A FUNCTION OF POWER LEVEL AND CO₂ FLOW

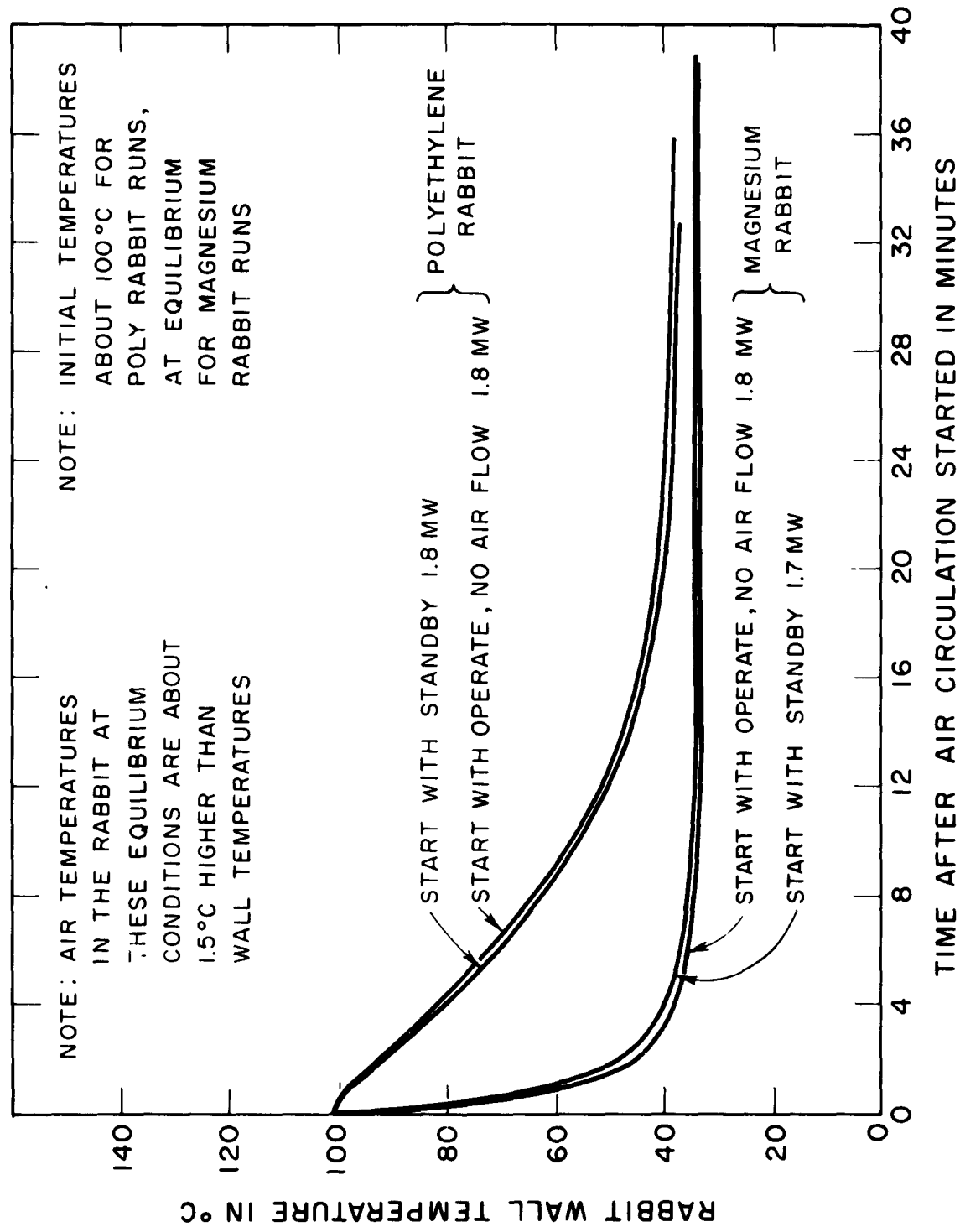


FIG. 22 EFFECT OF FULL AIR CIRCULATION ON RABBIT TEMPERATURES

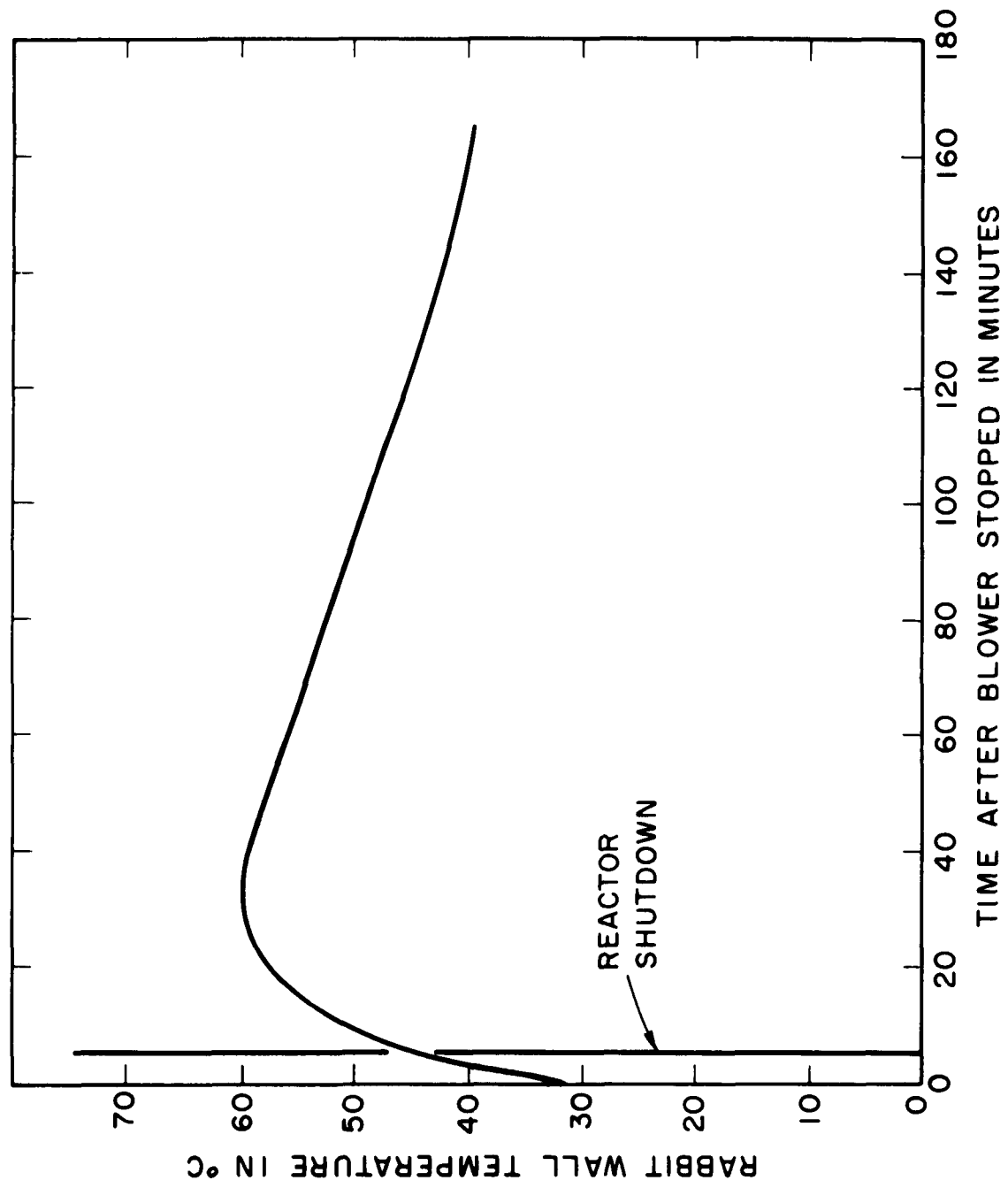


FIG. 23 RABBIT TEMPERATURES AFTER REACTOR SHUTDOWN

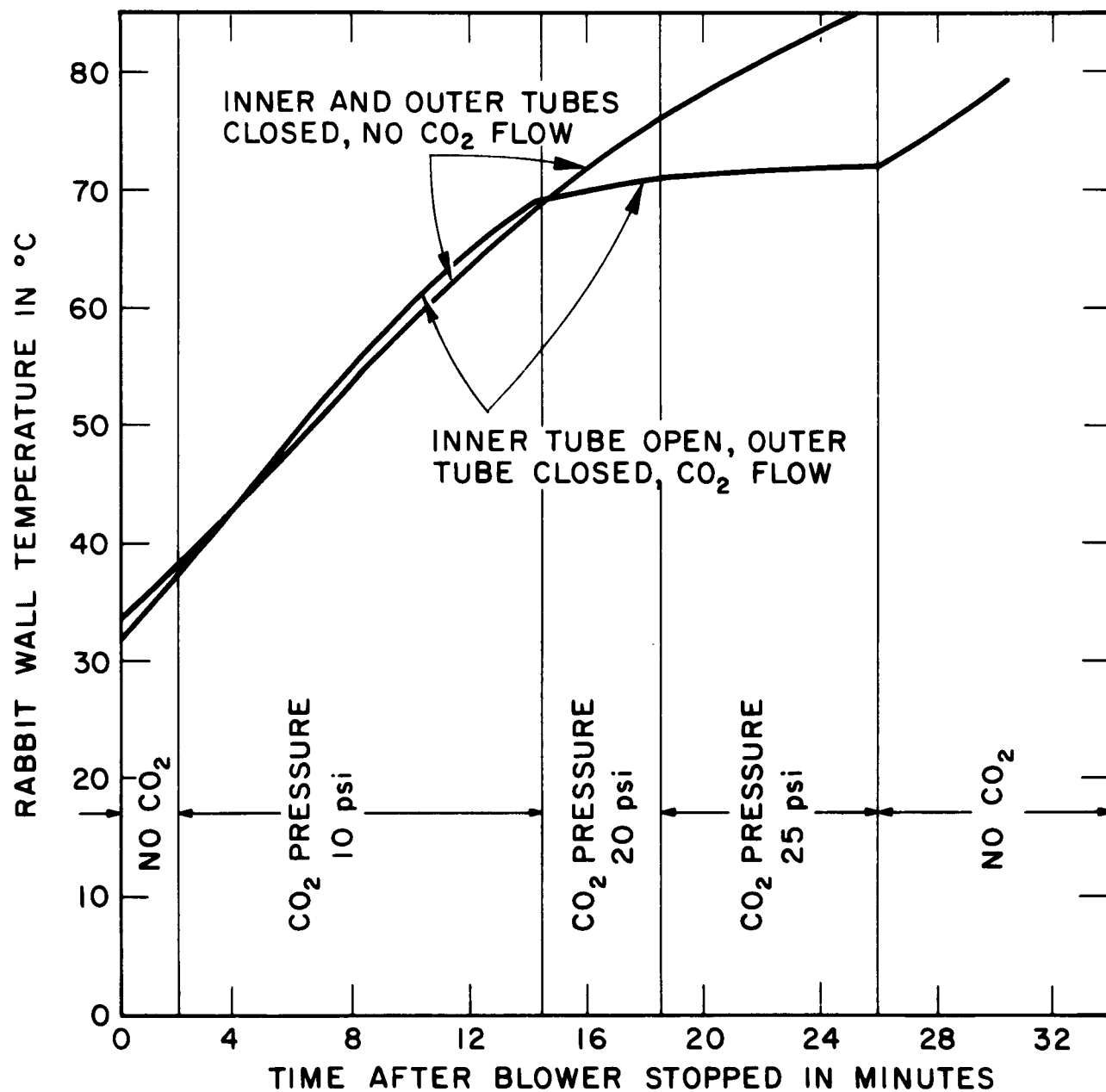


FIG. 24 RABBIT EMERGENCY COOLING TEST

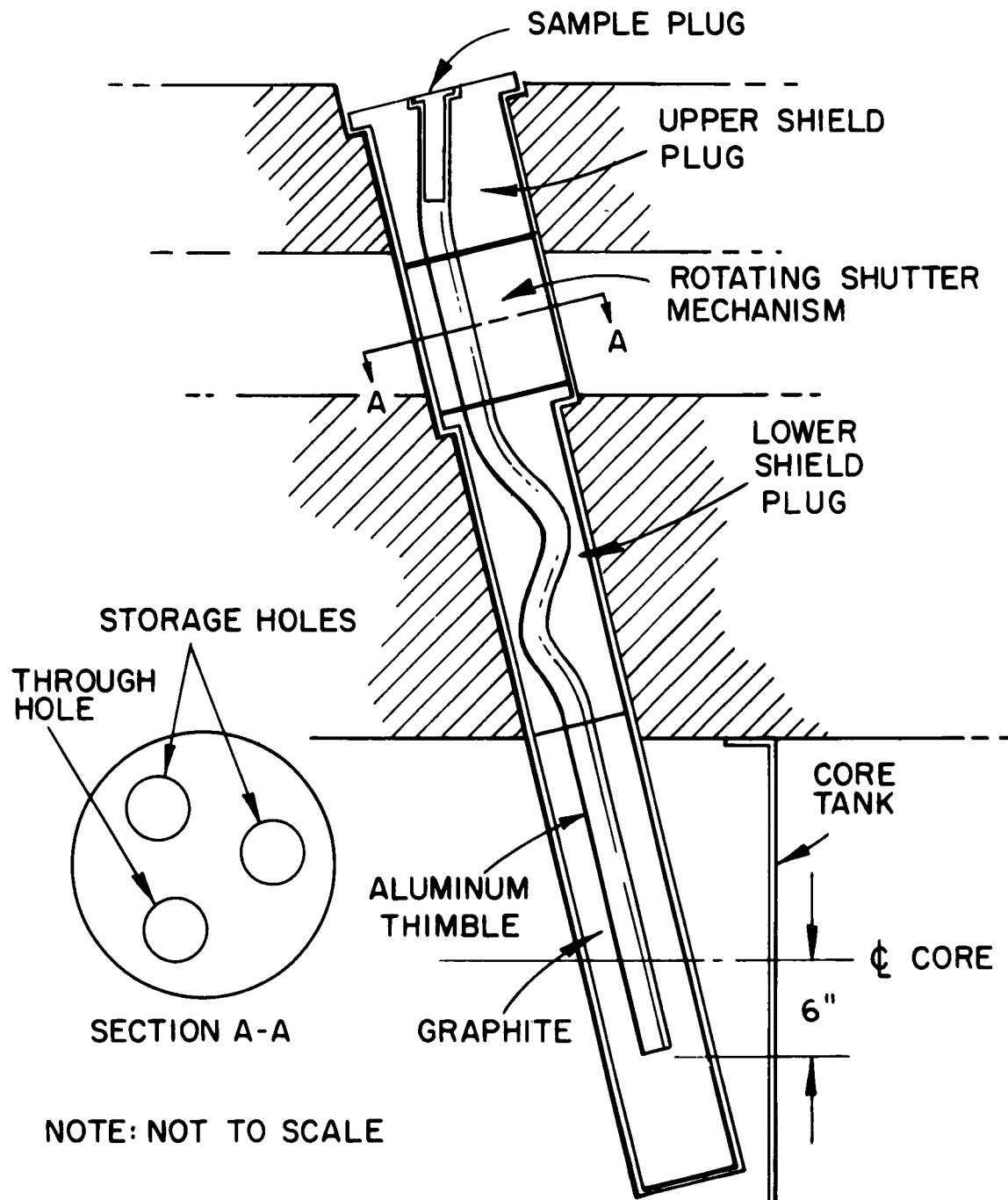
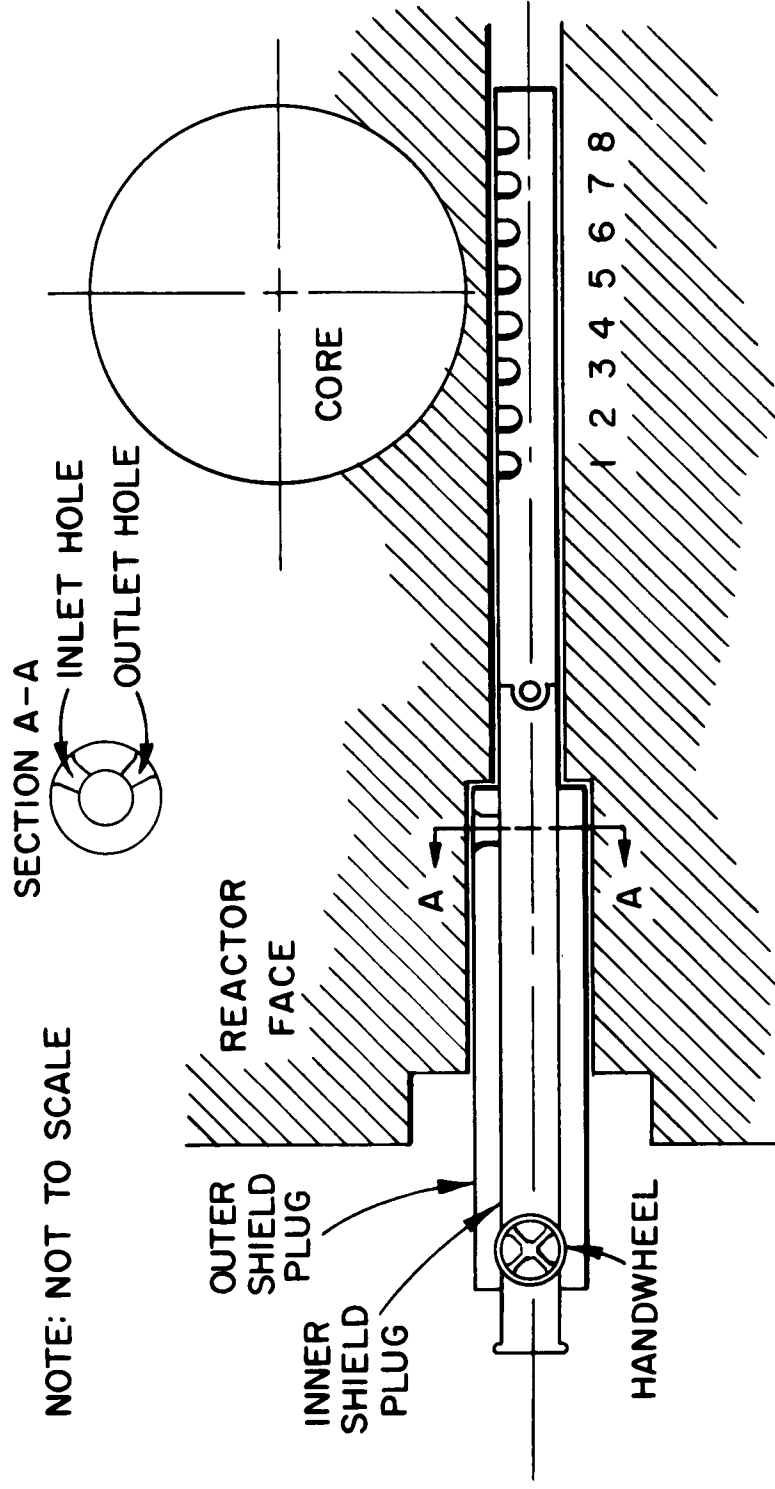


FIG.25 VERTICAL SAMPLE CHANGING FACILITY
(3GV5)



HOLE NUMBER	1	2	3	4	5	6	7	8
DISTANCE FROM CORE	8 3/4"	6 1/2"	4 1/4"	2"	1/4"	2 1/2"	4 3/4"	7"

FIG. 26 BALL SAMPLE CHANGER FACILITY (4TH1)